

Link Adaptation Criteria for Multicarrier Signaling on Doubly-selective Wireless Channels

Martina Angelone

December 16, 2008

Contents

| | | |
|----------|--|-----------|
| 1 | Introduction | 1 |
| 2 | System Model | 5 |
| 2.1 | FEC coding | 7 |
| 2.2 | Interleaver | 8 |
| 2.3 | Modulation and coding schemes (MCS) | 8 |
| 2.4 | OFDM system | 9 |
| 2.5 | Channel model | 11 |
| 2.6 | Channel state information | 14 |
| 2.7 | Simulations results | 14 |
| 3 | WER estimate | 19 |
| 3.1 | Effective SNR mapping | 20 |
| 3.2 | State of the art | 22 |
| 3.2.1 | Rayleigh channel hypothesis | 29 |
| 3.2.2 | Other methods | 31 |
| 3.2.3 | Performances | 34 |
| 4 | Link Adaptation and HARQ | 45 |
| 4.1 | Link Adaptation | 45 |
| 4.1.1 | Adaptation algorithm | 46 |
| 4.1.2 | Link adaptation performances with various ESM criteria | 48 |
| 4.2 | Hybrid automatic repeat request (HARQ) | 56 |
| 4.2.1 | Retransmission results | 57 |
| 5 | Conclusions | 61 |

*A Marta,
con tutto l'affetto e l'amicizia
che avrei ancora voluto darti.*

Chapter 1

Introduction

Exchanging information between people all around the world is one of the technologies' frontiers of this century. This is possible by wireless communications that, thanks to their flexibility and scalability are overcoming the market. The motto "be connected everywhere, every time and with everyone" describes as much as ever the users' demand for new wireless and mobile systems that can satisfy the future needs of broadband communications. Convergence in the wireless access network will also allow to simplify and lower the cost associated with today's complex networks, which have traditionally carried voice, data and video traffic on separate paths. Therefore wireless communication technologies are becoming a segment in continuous growth and of big interest for many telecommunication industries.

By now, wireless communications have been classified and fragmented in different segments, depending on the applications and on the linked requirements. On the horizon of advanced research we starve to integrate the voice service with data transmission, maintaining a good quality of service. Anyway, due to the diversity of requirements, integrating different services on the same wireless network still represents challenge. Voice service, which by now has been supported by UMTS, requires high QoS, minimum delay but relatively low data rates, while data transmission uses high data rates and, though being delay tolerant, it is strongly error intolerant. Moreover, if we think about multimedia traffic such as real time video it is clear that such applications are even strongly delay intolerant.

The next wireless communication standards will have to trade off those characteristics. An example of these standardizations is the IEEE 802.16 for fixed and mobile broadband wireless access, known also as WiMAX, which will be soon in competition with the evolved UMTS radio access network or 3GPP Long Term Evolution

(3GPP-LTE) [1].

The main goal of the next generation communication systems is then that of offering to the user a fast, reliable and flexible connection, suitable for many different contexts. To guarantee those requirements, the networks must be designed to handle the very bursty and unpredictable nature of packet-based traffic. Moreover, if we think of using wireless as the primary connection resource in a metropolitan context, we have to face with the different delays deriving by the various geometry and obstacles of the environment.

Bandwidth costs money, so the networks providers want to use it as effectively as they can, thus the goal is to reach the highest possible data rate given a certain bandwidth. One of the key elements which allows us to ensure that users constantly receive the fastest data rate, is the adaptation of the transmission scheme to channel conditions. The idea of adapting the modulation to the link status was proposed a few decades ago by J.F. Hayes [2]. In [3] it is shown that, for broadband wireless communication systems, substantial performance improvement can be achieved by adaptive modulation. This *link adaptation* accommodates varying conditions that can often occur on the radio link, as interference from buildings or trees or fading of the signal due to the user going away from the base station and represent therefore a general solution to optimize bandwidth usage.

To adapt it is fundamental to have some channel state information (CSI) which characterizes our transmission environment. Given this, we have to wonder which should be the next step towards link adaptation. In other words, we must choose a channel metric and a function of it on which our adaptation criteria should rely on. One of the most significant parameter in wireless transmission is the WER (Word Error Rate), known also as PER (Packet Error Rate) which allows us to establish the conditions over which our system must be considered “out of service”. This parameter is the most significant to evaluate the QoS of a transmission system, as imposing certain QoS constrains means choosing an adaptation policy that guarantees the target WER for the system. For this reason, the first goal of our work is trying to find an *estimate* of the WER, that will constitute the core of the adaptation criteria, basing on the CSI present at the transmitter.

We suppose to have perfect channel state information, so that there is no need of channel estimate algorithm. Anyway we still have to consider the WER estimate error that may induce the transmitter to chose a set of transmission parameters

which cannot guarantee the required QoS as the receiver cannot decode correctly some codewords: in that case, it would be fine to apply *retransmission*.

We introduce therefore the automatic repeat request (ARQ) as a complementary technology that can be often used together with LA to improve the total QoS of our system. A good example for this technologies union is the high speed downlink packet access (HSDPA) which is standardized as an element of the 3rd generation partnership project (3GPP) Release 5 specification. In ARQ the retransmission is accomplished with a standard protocol where, if a packet cannot be decoded it is discarded and entirely retransmitted again. A variation of standard ARQ is called hybrid ARQ scheme, in which the retransmission is combined with FEC. In this way it is easy to improve the success of decoding with a lower number of retransmissions than in the standard ARQ [5].

In this thesis we intend to investigate the technology of link adaptation (LA) trying to improve its performances from the base, which is the word error rate estimate. To get better results we further apply also hybrid automatic repeat request (HARQ).

Our work was carried out in the radio access laboratory of Centre Tecnologic de Telecomunicacions de Catalunya (CTTC). We used the MATLAB simulator to study the trend of the WER resulting from various channel conditions and then to evaluate the performances of the developed transmission system. The thesis is structured as follows. First of all, in chapter 2, we describe our system model and its components to better define the problem context. Then, in chapter 3, we introduce the WER estimate issue, describing the state of the art and introducing a quite reliable algorithm based on a new estimate method. In chapter 4 we pass to the real adaptation step, that allows us to finally evaluate the performances of each estimate algorithm. To complete the discussion, we describe the HARQ characteristics and show its benefits as a complement of link adaptation. In the conclusions, we summarize the whole work, pointing out some possible open issues.

Chapter 2

System Model

To introduce our problem, we first have to define the system model that has been used as a reference for our simulator.

Over the past several years, the Orthogonal frequency division multiplexing (OFDM) [6] technology has been successfully used in many applications such as broadcasting (i.e. DVB), wireless WLAN, WiMAX and wireline asynchronous digital subscriber line (ADSL). This technology is an effective signaling technique for overcoming the effects of frequency selective fading in broadband wireless communication channels. As we are facing with the problem of a high frequency selectivity, we want to exploit its intrinsic ability to handle fading channels, as we will better explain later.

The investigated OFDM system scheme is shown in Figure 2.1

As we can see from the structure, the coding and modulation are distinct operations. This is because we chose as our transmission scheme the bit-interleaved coded modulation (BICM) [7]. The term BICM arises from the fact that the coded bits that are interleaved before the modulation but after the coding process. This differs from the common interleaving process, where the encoded symbols themselves are interleaved to obtain independent channel fades. Bit interleaved coded modulation involves combining a low rate code with a higher order signal constellation. This topic has become of significant research interests in recent years as attention on practical coding and modulation for wireless fading channels has intensified. The combination of BICM and OFDM is a very effective technique to exploit the diversity that is intrinsic of the frequency selective fading channels.

For the moment, we introduce the simplified signal model that will be used throughout the whole thesis, whose justifications will be better explained later in the next

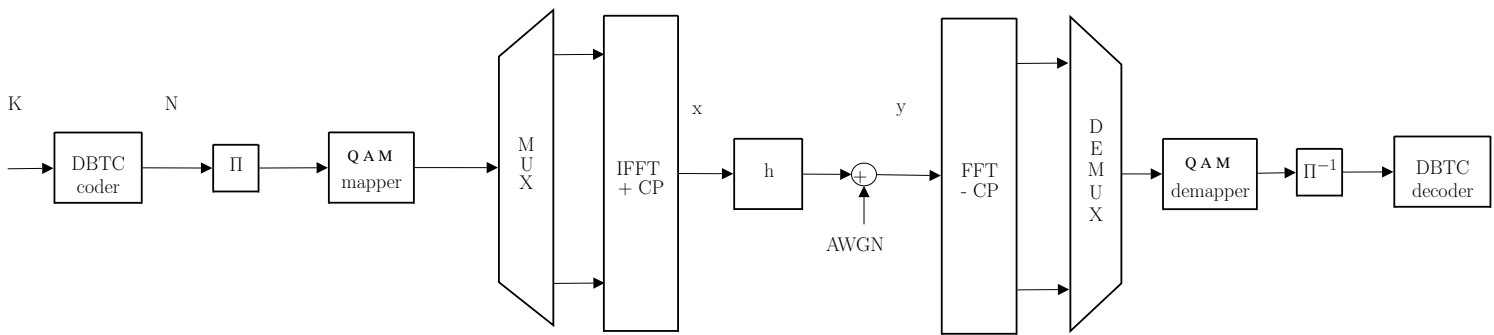


Figure 2.1: Transmission system model

paragraphs. Thanks to some hypothesis on the OFDM parameters, we denote with x the encoded and modulated transmitted signal after the IFFT operation and we can therefore define the received signal as

$$y = h \cdot x + w \tag{2.1}$$

with $h \sim \mathcal{CN}(0, 1)$ and $w \sim \mathcal{CN}(0, N_0)$, while N_0 indicates the monolateral spectral density of the noise. We then suppose to deal with the data flow of a single user transmitted by a single antenna with a normalized energy per QAM symbol

$$E_s = \mathbb{E}[| x |^2] \tag{2.2}$$

The *average* SNR used for the transmission is given by

$$\bar{\gamma} \triangleq \mathbb{E}[| h |^2] \frac{E_s}{N_0} = \frac{E_s}{N_0} \tag{2.3}$$

We now examine each component of our model.

2.1 FEC coding

Forward error-correction coding (FEC), also called channel coding, is a type of digital signal processing that improves data reliability by introducing redundant bits. This structure enables the receiver to detect and possibly correct errors caused by corruption from the channel. The decoder is then able to correct errors without requesting retransmission of the original information. In a communication system that employs FEC coding, a digital information source sends a data sequence to the encoder. This one inserts redundant (or parity) bits, outputting a longer sequence of coded bits. In block codes we can determine a finite sequence of output encoded bits: this is what we will refer to as a *codeword*. The coefficient R_2 that links the codeword length N with the number of information bits originally transmitted K is called *code rate* and can be defined as

$$R_2 = \frac{K}{N} \tag{2.4}$$

It's easy to see that in any case $R_2 \leq 1$.

Codes that introduce a big amount redundancy convey relatively little information per each individual coded bit and this fact reduces the probability of having an error on the original data. On the other hand, the addition of parity bits will generally increase transmission bandwidth requirements or anyway reduce the throughput for

a given bandwidth.

In our system we will use a turbo code, which is well known for ensuring robust communications despite adverse conditions. In particular, we adopt a double-binary turbo encoder (DBTC) [8], [9] rate compatible that provide a good flexibility in terms of block lengths and code rates. This type of encoder differs from the simple turbo code by the fact that the information bits are encoded pair wise. At the receiver, a soft demapper derives an a posteriori probability (APP) L-value for each received coded bit and then passes those values to the de-interleaver and finally to the decoder. We therefore speak of APP soft demapping at the receiver side.

The DBTC shows good performances already at quite low block sizes and therefore we choose the info-bits packet length of $K = 288$. The coderate can be obtained by puncturing and, when adapting, we can chose among those possible values:

$$R_2 = \left\{ \frac{1}{3}, \frac{1}{2}, \frac{2}{3}, \frac{6}{7} \right\} \quad (2.5)$$

each one will be later associated to a certain modulation.

In conclusion, the first block of our system substantially groups the flow of information bits into packets of K bits, which are then encoded with a coding rate R_2 to obtain the correspondent codewords, each one constituted of N coded bits.

2.2 Interleaver

Interleaving is a process of scrambling the order of a data sequence, in our case of the codeword, to enhance the error correcting capability of decoding [7]. This is possible because this technique actually spreads out the burst errors. Inserting the interleaver after the coder we have a bit interleaved turbo coded modulation and this scheme, together with the double-binary turbo code, allows us to achieve low complexity and excellent WER performance [10]. The inverse of this process is called deinterleaving, which restores the received sequence to its original order.

In our system we use a random interleaver, which permutes the bits within each codeword in a random way and allows us to use a bit interleaved coded modulation.

2.3 Modulation and coding schemes (MCS)

The successive block is constituted by the QAM mapper. As we said before, in the BICM scheme the coding and the modulation are separated steps.

The coded and interleaved bits of each codeword are simply mapped to constellation

| MCS c | 1 | 2 | 3 | 4 | 5 | 6 | 7 |
|-------------|-----|-----|-----|-----|-----|-----|-----|
| $R_1^{(c)}$ | 2 | 2 | 4 | 4 | 4 | 6 | 6 |
| $R_2^{(c)}$ | 1/3 | 1/2 | 1/3 | 1/2 | 2/3 | 2/3 | 6/7 |

Table 2.1: MCS set specification

elements belonging to a certain QAM modulation scheme. Denoting with R_1 the modulation order (number of bits per QAM symbol), we define our set of modulation and coding schemes (MCS) that will be used in our system, evaluating their performances for various combinations of the constellation size and the codeword length.

In [11] it is indicated the best set of MCS that we should chose for our adaptation system. The reference curves are obtained simulating over an AWGN channel and implementing all constellations between QPSK and 64QAM. We apply Gray labeling to the square constellations and quasi-Gray to the non-square ones. Simulations results show that the throughput of non-square constellations is almost always below that of the squared constellations and therefore we can exclude MCS deriving from 8-PSK, 32-QAM and 128-QAM. Taking into account those considerations, we are now able to define the modulation and coding set that is shown in Table 2.1. With the index $c = 1, \dots, 7$ we denote each MCS.

As we will better see later, after the adaptation algorithm one of those MCS is selected as the transmission scheme for transmitting in the particular channel condition. In conclusion, for a given a modulation scheme we associate one M-QAM symbol to every $R_1 = \log_2(M)$ coded bits and therefore we have a total number of $N_q = \frac{K}{R_1 \cdot R_2}$ QAM symbols per codeword, where K is fixed and equal to 288. For an AWGN channel, we can easily demonstrate that the spectral efficiency is given by the product $R_1 \cdot R_2$. It's easy to see that, for a fixed length of K , the higher is the spectral efficiency of the selected MCS, the less number of symbols are necessary to map a codeword.

2.4 OFDM system

During a transmission, the wide band signal arrives at the receiver using various paths of different lengths and for this reason it is subject to considerable distortions

due to the propagation on those multi-paths. Since multiple versions of the signal interfere with each other, it rises the so called inter symbol interference (ISI) and in these conditions it becomes very hard to extract the original information.

The issue of the frequency selectivity is then due to the fact that the transmitted signal band is wider or comparable with the inverse of the delays present among the various multi-paths, that we use to call band of coherence of the channel.

Orthogonal frequency division multiplexing is a multi-carrier modulation [3] that divides the data stream into multiple substreams which are then transmitted over different orthogonal subchannels. Each subchannel is centered on different subcarrier frequencies, which are spaced so that it's guaranteed the "orthogonality". Indicating with N_c the number of these subcarriers, what we actually do is modulating each substream with a narrow band signal, so that each of them "sees" a flat portion of the channel spectrum as it has a bandwidth lower than the channel coherence bandwidth. In other words, the number of those substreams is chosen to make the symbol duration on each substream much greater than the delay spread of the channel.

Considering a system with baseband bandwidth B , the resulting bandwidth on each subcarrier is $B_N = B/N_c$ and, to ensure a relatively flat-fading on each subchannel, this has to be much lower than the coherence bandwidth of the channel B_c .

The implementation of the OFDM system is shown in Fig. 2.1. As we can see, after the QAM mapper the signal is divided into multiple streams with a multiplexer, then each stream is processed with an IFFT and transmitted.

In particular, we also add the so called cyclic prefix (CP) which has a duration T_g named guard interval that is bigger than the finite duration of the channel impulse response T_h . This insures that each OFDM symbol (constituted by the N_c subcarriers) will not experience significant ISI as we avoid every possible overlapping.

We then assume that the OFDM system is simulated in the frequency domain, without explicitly simulating the IFFT and FFT processing nor the cyclic prefix. Supposing that actually in our system it is $T_h \leq T_g$ we can consider the channel coefficient on each subcarrier independent from the others and this hypothesis allows us to ignore the implementation details of the OFDM system.

Our system model can be therefore considered the one depicted in Figure 2.2 in which we have independent channel coefficients for each substream with additive Gaussian noise. The number of used subcarrier is $N_c = 1024$.

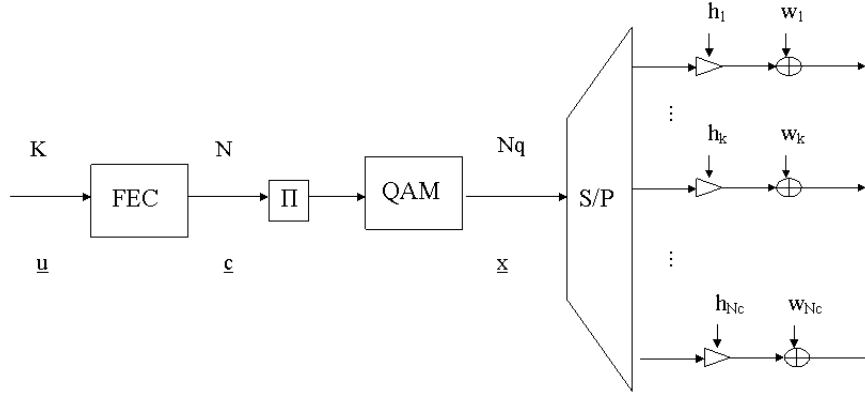


Figure 2.2: Equivalent block scheme of the transmitter

2.5 Channel model

We can see all the described operations referring to the vector \underline{u} containing the packet of infobits $\underline{u} = [u_1, u_2 \dots, u_K]$ which is first coded into $\underline{c} = [c_1, c_2 \dots, c_N]$ and then mapped onto QAM symbols, as indicated still in Figure 2.2. After the OFDM, which in our hypothesis simply corresponds to a serial to parallel conversion, N_c QAM symbols are transmitted, forming one OFDM symbol that can be described with the vector $\underline{x} = [x_1, x_2 \dots, x_{N_c}]$.

At the receiver, each received symbol y_k , $k = 1, \dots, N_c$ can be considered belonging to a single carrier system, with a certain coefficient for the channel fading and for the additive noise. This is :

$$y_k = h_k \cdot x_k + w_k \quad \text{for } k = 1 \dots N_c \quad (2.6)$$

where the coefficient h_k represents the channel fading on the k -th subcarrier and w_k is the additive noise on that subcarrier.

Supposing to have a non-line-of-sight scenario, the complex fading coefficients on each subcarrier are the result of the sum of many coefficients coming from multiple signal contributions. Those contributions derive in fact from the multipath environment and each one of them has its own delay and fade value. As the number of the contributions is high, we can apply the central limit theorem and say that the resulting fading coefficient value (both real and imaginary part) belongs to a Gaussian distribution. We therefore have N_c independent channel coefficients that can be described as a *complex gaussian* random variable with variance $\sigma_h^2 = 1$, while the noise coefficients w_k belongs to a Gaussian normal distribution:

$$h_k \sim \mathcal{CN}(0, 1), \quad \text{for } k = 1 \dots N_c \quad (2.7)$$

$$w_k \sim \mathcal{CN}(0, N_0), \quad \text{for } k = 1 \dots N_c \quad (2.8)$$

In literature such a channel is known as Rayleigh channel, as the absolute value $|h_k|$ has a Rayleigh distribution with parameter σ equal to the standard deviation per real dimension of the variable h_k , or $\sigma = \frac{1}{\sqrt{2}}$, whose probability distribution function is that of (2.9) and it is shown in Figure 2.3

$$p(|h_k|) = \frac{|h_k|}{\sigma^2} \cdot \exp\left(-\frac{|h_k|^2}{2\sigma^2}\right), \quad x \geq 0 \quad (2.9)$$

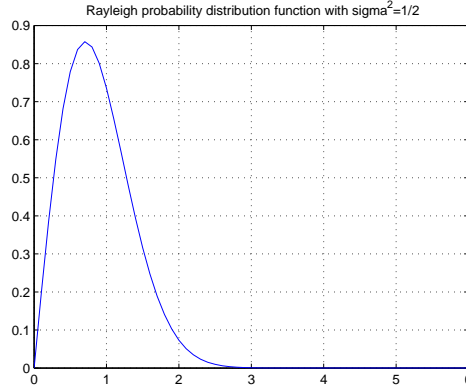


Figure 2.3: Rayleigh probability distribution function with $\sigma = \frac{1}{\sqrt{2}}$

We are now able to introduce the so called *instantaneous SNR* γ_k , which is the SNR seen by each subcarrier of our simulation. This is clearly a random variable, as it depends both from the deterministic mean SNR $\bar{\gamma}$ and from the absolute square value of the channel coefficient for each subcarrier $|h_k|^2$ through the relation:

$$\gamma_k = \bar{\gamma} \cdot |h_k|^2, \quad \text{for } k = 1 \dots N_c \quad (2.10)$$

where N_c , as we said, is the number of subcarriers per OFDM symbol. This variable has an exponential distribution with parameter $\bar{\gamma}$, as it's defined as the square module of a complex gaussian variable, that is h_k .

Our channel is then modeled as a blockfading channel.

In the frequency and time selective transmission environments, the channel transfer

function of the mobile channel changes from subcarrier to subcarrier in the frequency domain and from symbol to symbol in the time domain. In our model we assume that the channel realization remains the same during the transmission of a certain number OFDM symbols. Depending on the doppler frequency f_d of the user there is a possible range of values for the coherence time of the channel. Indicating it with τ_{coh} and with T_s our OFDM symbol duration, we have then $C = \lfloor \frac{\tau_{coh}}{T_s} \rfloor$ consecutive OFDM symbols with the same channel realization. We then refer to this block of C OFDM symbols as a *frame*.

Each channel realization is then modeled as a frequency selective channel, where the fading process is constant over blocks of n_B subcarriers, that corresponds to n_B QAM symbols, and then is drawn independently for the next group of subcarriers. This happens when the subchannel bandwidth has a proportional relation with the coherence band of the channel, which is in fact $n_B = \lfloor B_c/B_N \rfloor$. The model for increasing n_B represents a channel with sudden changes and is therefore a quite bad environment for the transmission, as there is more dependance from each single coefficient. In general we are therefore dealing with a doubly selective channel.

We illustrate below some examples of the described model basing on some specifics used in mobile WiMAX.

Coherence time is a parameter that describes the time varying nature of the channel. Supposing to work in the 2.3 Ghz band and to have an OFDM symbol duration of $102.86 \mu s$, as in the mobile WiMAX standard, we can formulate different problems depending on the relative motion between transmitter and receiver. For a pedestrian user that moves with a velocity of $3 m/s$, the coherence time is about $\tau_{coh} = 360 \mu s$ and therefore there are $C = 16$ OFDM symbols that experience the same channel realization, calculated as the floor integer of the quotient. Otherwise, if we consider a vehicular motion with a velocity of $50 m/s$, the channel impulse response is essentially invariant over at least $C = 3$ OFDM symbols.

On the other hand, delay spread and coherence bandwidth describe the time *dispersive* nature of the channel. Still referring to the mobile WiMAX specifics for the 1024 FFT case, we suppose to have the predefined subchannel bandwidth of $B_N = 10$ KHz. A typical delay spread in a wide outdoor area is $\Delta\tau = 1 \mu s$ and the resulting coherence bandwidth is $B_c = \lfloor \frac{0.05}{\Delta\tau} \rfloor = 50$ KHz. In these hypothesis, the number of correlated subcarrier is $n_B = 5$. Otherwise, if we take delay spread of $\Delta\tau = 5 \mu s$, that may be possible in rural areas, we have a very selective channel

with $n_B = 1$. This is an extreme case of fast fading in which each QAM symbol has a different channel coefficient. This case is often referred to as Rayleigh extreme fast-fading channel, or perfectly frequency interleaved channel. On the opposite extreme, we find $n_B = N_c$ which is the case called slow fading, as the entire code word is affected by the same fading coefficient.

In our simulations we will consider a scenario where the described parameters can assume a value among $C = \{1, 4, 16\}$ and $n_B = \{1, 4\}$, as those characteristics can represent realistic cases. In conclusion, we can state that our model is a doubly selective channel, as it has both a frequency selective fading and a time selectivity.

2.6 Channel state information

The knowledge of the characteristics of our transmission environment is an essential element for our adaptation aim. The frequency and time selectivity of the channel has to be considered in the design of the adaptation algorithm. In fact, first of all we must be able to recognize and catalogue the channel type in which we are operating. With channel state information (CSI) we then indicate the set of parameters useful to the transmission system for achieving this goal.

In particular, we want to realize a frame-wise adaptation applying the same modulation and coding scheme on all the subcarriers for the whole duration of the frame. The principal information needed is the knowledge of the channel transfer coefficients for all the subcarriers. Supposing that the channel is quasi-static for the duration of the frame (which is, as we said before, a block of C OFDM symbols) we assume to know the channel coefficients $h_k, k = 1, \dots, CN_c$. This context is known in literature as perfect CSI, as the receiver knows perfectly the channel coefficients. Exploiting those informations the receiver is able to chose the modulation and coding scheme that should be used for our transmission and then transmits back only this information to the transmitter through a feedback channel.

2.7 Simulations results

To validate the accuracy of our simulator we present in this section a set of simulation results.

Comparing in terms of word error rate (WER), we show the good fitting between some well known theoretical cases and the relative simulation results. The simplest hypothesis that we can do for our transmission, is to have an additive white gaussian

| c | $R_1^{(c)}$ | $R_2^{(c)}$ | $\gamma_0^{(c)}$ (dB) AWGN | $\alpha^{(c)}$ AWGN | $\gamma_0^{(c)}$ (dB) Ray | $\alpha^{(c)}$ Ray |
|---|-------------|-------------|----------------------------|---------------------|---------------------------|--------------------|
| 1 | 2 | 1/3 | -1.47 | 21.151 | -0.43 | 12.69 |
| 2 | 2 | 1/2 | 0.75 | 13.009 | 2.55 | 5.54 |
| 3 | 4 | 1/3 | 3.2 | 5.806 | 4.7 | 3.34 |
| 4 | 4 | 1/2 | 5.96 | 3.226 | 7.95 | 1.33 |
| 5 | 4 | 2/3 | 8.5 | 1.65 | 11.03 | 0.43 |
| 6 | 6 | 2/3 | 13.35 | 0.441 | 15.83 | 0.125 |
| 7 | 6 | 6/7 | 16.85 | 0.144 | 18.41 | 0.014 |

Table 2.2: $\gamma_0^{(c)}$ and $\alpha^{(c)}$ values for AWGN and Rayleigh channel

noise channel (AWGN), in which all the channel coefficients have the same value, that we suppose to be unitary.

Then, we can evaluate the trend of the opposite case relative to the Rayleigh extremely fast fading channel.

For comparing, we can either use some reference curves, taken from a database, or an analytical approximation based on the exponential function defined as:

$$p_w(\gamma) = \begin{cases} 1, & \text{if } \gamma \leq \gamma_0^{(c)} \\ \exp(\alpha^{(c)}(\gamma_0^{(c)} - \gamma)), & \text{if } \gamma > \gamma_0^{(c)} \end{cases} \quad (2.11)$$

where the parameters $\alpha^{(c)}$ and $\gamma_0^{(c)}$ are calculated for each modulation and coding scheme of Table 2.1 to guarantee a minimum quadratic approximation error [14] and are listed in Table 2.2 for both the channel types.

This analytical approximation is reliable if compared to the theoretical known expressions and shows a very good fitting with the simulation results. In Figure 2.4 and 2.5 we show this agreement, respectively for the gaussian and the Rayleigh fading channels.

Another extreme case that can be theoretically checked is that of the slow fading, in which the entire OFDM symbol is affected by the same fading coefficient, as $n_B = N_c$. This case can be seen as if we had an AWGN channel with a different realization for each OFDM symbol. Therefore we can derive the theoretical expression for the word error rate of this channel simply calculating the expectation of the WER given in (2.11) averaged with the probability distribution function of the aleatory variable

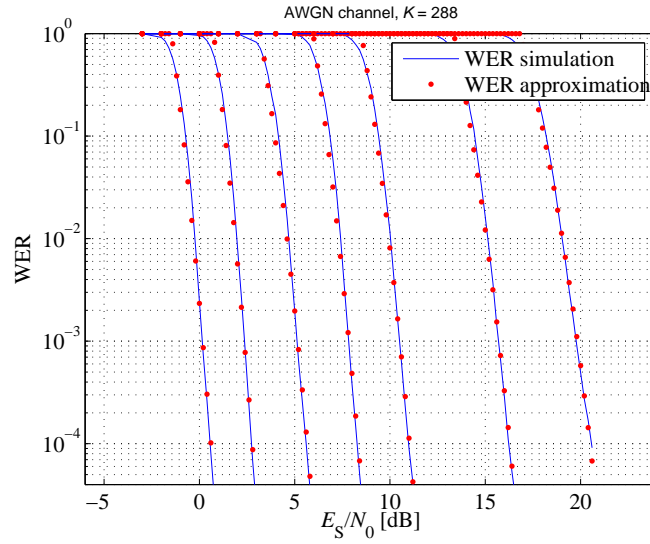


Figure 2.4: Fitting between analytical approximation and simulation results of the WER for AWGN channel

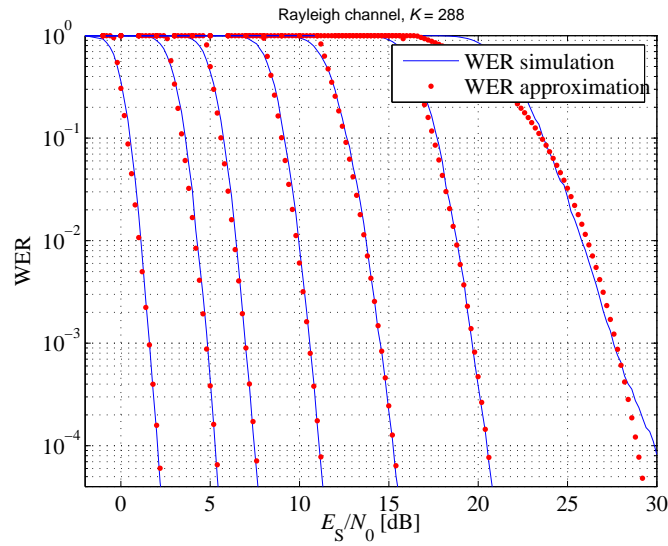


Figure 2.5: Fitting between analytical approximation and simulation results of the WER for Rayleigh fast fading channel

γ_k that is, as we said, an exponential variable. In formulas:

$$\begin{aligned}
WER(\bar{\gamma}) &= E[WER_{AWGN}(\gamma_k)] \\
&= \int WER_{AWGN}(\gamma) \cdot f_{\gamma_k}(\gamma) d\gamma
\end{aligned} \tag{2.12}$$

The result of this operation is this closed form:

$$WER(\bar{\gamma}) = 1 - \exp\left(\frac{-\gamma_0}{\bar{\gamma}}\right) + \frac{\exp\left(\frac{-\gamma_0}{\bar{\gamma}}\right)}{\bar{\gamma}\left(\alpha + \frac{1}{\bar{\gamma}}\right)} \tag{2.13}$$

Also for this theoretical expression, simulation results in Figure 2.6 show a very good agreement.

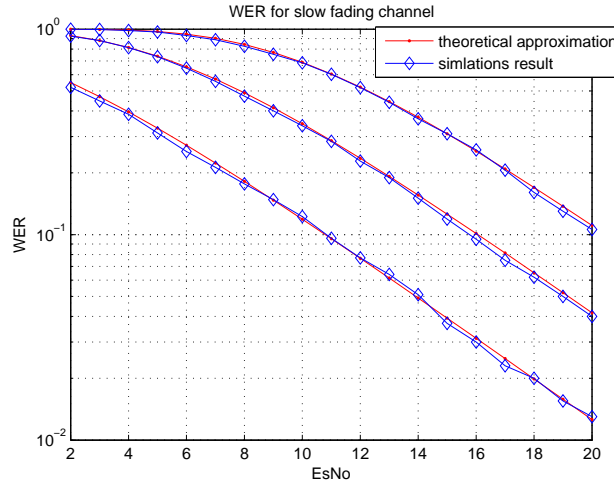


Figure 2.6: Fitting between analytical approximation and simulation results of the WER for Rayleigh slow fading channel

Chapter 3

WER estimate

Usually, the performances of a radio link are evaluated in terms of WER in function of the mean SNR used for the transmission, averaging over many realizations of a certain channel model. Nevertheless, the specific channel realization encountered by the transmitted packets can give rise to a performance curve significantly different from the averaged one. For this reason, if we want to apply link adaptation, we need an accurate link performance model that takes into account the instantaneous channel conditions.

We suppose to work in a context where the QoS is mainly evaluated in terms of word error rate. This means that we have a constraint on the possible maximum value that the WER could reach, which represents the WER_{max} . In our simulations we tolerate to have one error over 100 received codewords, that corresponds to a $WER_{max} = 10^{-2}$. Once fixed this limit, it is clear that, to reach our adaptation goal, we have to know the real trend of the WER on our channel for each frame and for each modulation and coding scheme, among which we have to select the transmission parameters. In fact, the knowledge of the WER allows us to establish which MCS, for a given mean SNR, respects the WER constraint maximizing the throughput.

Therefore, to proceed with link adaptation, we first need a physical layer (PHY) abstraction that estimates link layer performance in terms of WER, using an accurate and computationally simple estimate algorithm [15]. This algorithm should be independent from the channel model and therefore we try to find a possibly suitable solution for every variant of our doubly-selective channel.

The WER trend is well known for the ideal additive white Gaussian noise channel and for the extremely selective Rayleigh fading, whose expressions can be easily

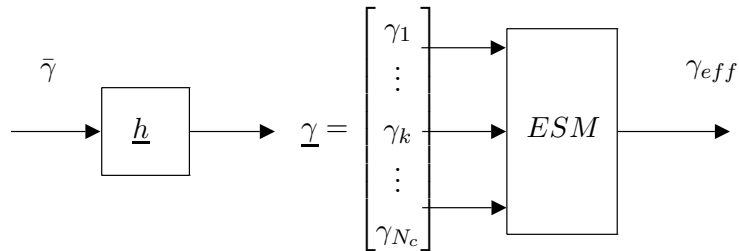


Figure 3.1:

approximated with (2.11). For the intermediate cases, if we want to do adaptation, we need an *estimate* of the WER. For this reason, the main point of our work lies in the WER estimate algorithm.

3.1 Effective SNR mapping

The role of a PHY abstraction method is to estimate the word error rate for a given channel realization across the OFDM subcarriers. In fact, the abstraction consists of a link level simulation that has the channel scenario as input. This simulation has the main purpose of generating SNR-WER look-up tables that are able to take into account the fast fading statistics exploiting instantaneous channel conditions [16]. Therefore, to exploit the channel variability and its information, we have to define a scalar metric which associates to every mean SNR at the transmitter side, the so called *effective* SNR. This operation, termed Effective SNR Mapping (ESM) has been widely studied in literature and consists in a compression of the vector of instantaneous channel SNR values to a single effective SNR value that we indicate as γ_{eff} , which can then be further mapped to a WER number.

We define the vector of instantaneous SNRs $\underline{\gamma} = [\gamma_1, \gamma_2 \dots \gamma_k \dots, \gamma_{N_c}]$ which, as we already said, are given by:

$$\gamma_k = \bar{\gamma} \cdot |h_k|^2, \quad for \ k = 1 \dots N_c \quad (3.1)$$

and show a scheme of the estimate procedure in Figure 3.1.

If an analytical approximation expression is available, the result of this operation can be interpreted also as an interpolation, with the γ_{eff} values, onto a reference WER curve, plotting the result in function of the initial SNR $\bar{\gamma}$, as shown in Fig.3.2 and 3.3

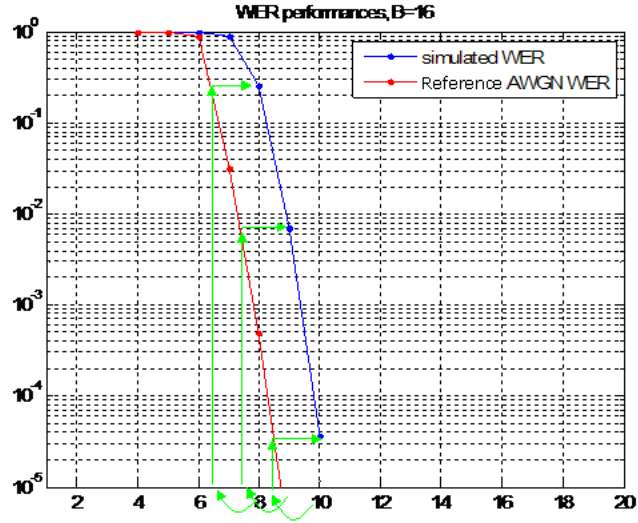


Figure 3.2: Interpolation with $\gamma_{eff} < \bar{\gamma}$

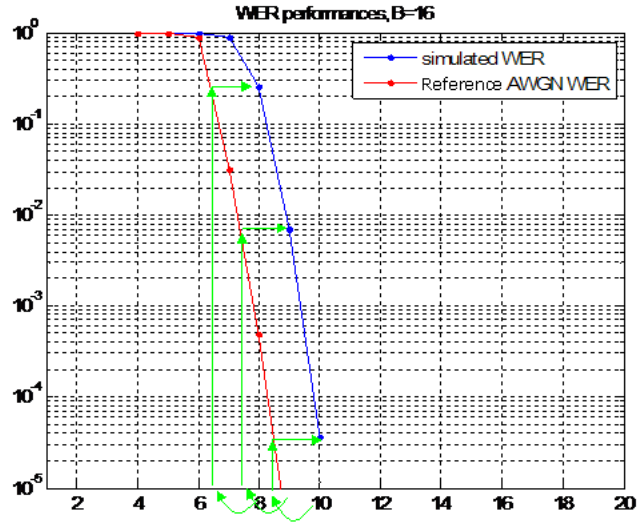


Figure 3.3: Interpolation with $\gamma_{eff} > \bar{\gamma}$

Indicating the known WER curve of reference as WER_{ref} , we can summarize the estimate algorithm with the equation:

$$\widehat{WER}(\bar{\gamma}) = WER_{ref}(\gamma_{eff}) \quad (3.2)$$

where $\widehat{WER}(\bar{\gamma})$ is our estimate in function of the transmission's SNR.

We now focus on defining how to derive the γ_{eff} value. Assuming to have perfect channel state information, we calculate the capacity of a selective channel as:

$$I(\gamma_{eff}) = \int I(\gamma) f_{\gamma_k}(\gamma) d\gamma \quad (3.3)$$

where $f_{SNR}(\gamma)$ is the probability distribution function of the random variables belonging to the vector of instantaneous SNRs $\underline{\gamma}$, which have, as we said, an exponential distribution. The mapping operation is derived in [18] from the above equation, defining the general form:

$$\gamma_{eff} = I^{-1}\left(\frac{1}{N_c} \sum_{k=1}^{N_c} I(\gamma_k)\right) \quad (3.4)$$

where we generally denote the function $I(\cdot)$ as “information measure”, though it can be a general function, and $I(\cdot)^{-1}$ its inverse. The choice of this function is a crucial point in the WER estimate as it characterizes the channel capacity.

The goodness of the function $I(\cdot)$ that, for every mean SNR $\bar{\gamma}$, maps the vector of γ_k into the scalar value of effective SNR γ_{eff} , is given by the estimate error between the simulated WER and the estimated one, \widehat{WER} . This estimate error is given by the average on the values deriving from (3.5) calculated for every mean SNR $\bar{\gamma}$:

$$\varepsilon = \frac{(\widehat{WER} - WER)^2}{WER^2} \quad (3.5)$$

3.2 State of the art

In the past, several ESM approaches to predict the instantaneous link performance have been proposed in literature. The link level curves have been generated assuming a frequency flat channel response at given SNR. This means that, to create the look-up tables, as well as from the interpolation point of view, the Gaussian channel WER is the reference curve to do the mapping, or in other words $WER_{ref} \equiv WER_{AWGN}$. Summing up, we have to map the instantaneous channel state of γ_k , for $k = 1 \dots N_c$ into an effective SNR γ_{eff} , and use it to find an estimate of the WER from basic AWGN link-level performance. In this context, where our reference is the Gaussian channel, we can state that the ESM is sufficiently accurate if we obtain:

$$\widehat{WER}(\bar{\gamma}) = WER_{AWGN}(\gamma_{eff}) \approx WER(\bar{\gamma}) \quad (3.6)$$

where $WER(\gamma)$ is the real word error rate experienced by the transmission on the particular channel realization and $\widehat{WER}(\bar{\gamma})$ is our estimate result. To achieve efficient link adaptation, this relation has to be fulfilled for each channel realization that we experience during our transmission.

As we said, in literature there have been studied several functions to perform ESM. In many of them, it is used a scaling factor, different for each MCS, that allows to optimize the estimation performance adjusting the trend of the estimated WER with a “least square fit” criterium [17].

In our work we don’t use any kind of scaling factor, as we propose to compare and investigate some already present methods with each other and also with some possible new solutions with a suboptimum approach, without evaluating the unfair advantages deriving from such a treatment.

Moreover, in many papers it is demonstrated that the main and more reliable method to obtain accurate estimate is based on the mutual information ESM and is called MIESM. Nevertheless, the mutual information function is a non-closed form and requires therefore the construction of a look up table numerically calculated. To avoid these calculations we use the suboptimum approximation for the mutual information function which is given, as we will describe later, by the capacity formula for the Gaussian channel.

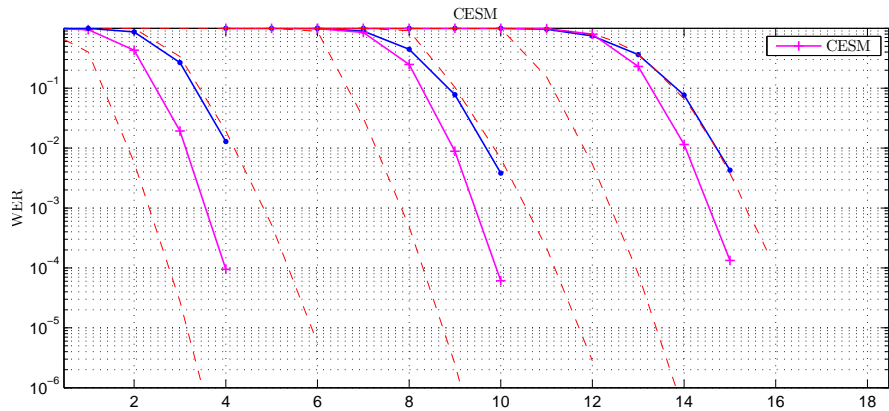
We now introduce some commonly known link performance models that differs from each other in the ESM function of information measure.

Capacity effective SNR mapping (CESM) The simplest metric that is suggested by our “information measure” approach is the *capacity*, as explained in the following considerations.

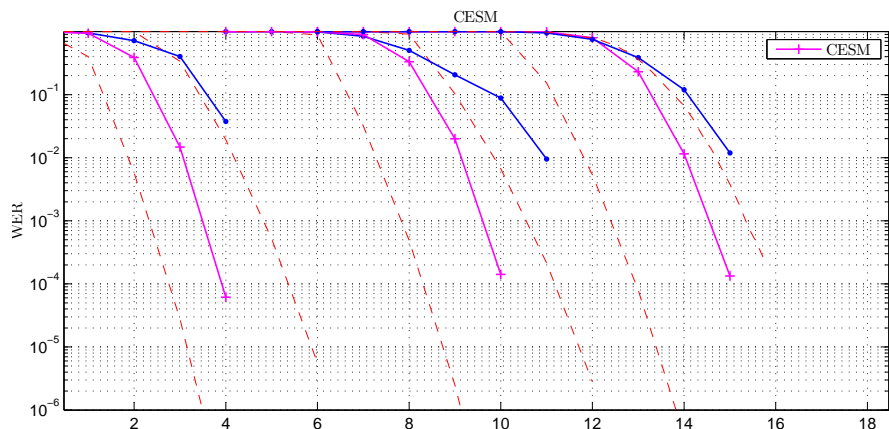
Supposing to have an OFDM system with a subchannel bandwidth sufficiently narrow in confront of that of the frequency selective channel, it is reasonable to think that each subchannel sees a flat fading and therefore we are able to calculate its particular Gaussian capacity with the well known formula:

$$C_k = \log_2(1 + \gamma_k) \quad \text{for } k = 1 \dots N_c \quad (3.7)$$

Then, this set of instantaneous capacities is averaged on the number of subcarriers, so that the final value is a sort of mean capacity that characterizes the particular channel realization. Finally, the idea is to obtain an effective SNR that corresponds to this value, as if the whole channel had this mean capacity. This reasoning leads



(a) $n_B = 1$



(b) $n_B = 4$

Figure 3.4: CSM performances for QPSK, 16QAM and 64QAM with $R_2 = 0.5$ and $n_B = 1, 4$. Dashed lines represent the AWGN and Rayleigh theoretical curves for each modulation

us again to formula (3.4), as the final effective SNR is given by

$$\gamma_{eff} = C^{-1} \left(\frac{1}{N_c} \sum_{k=1}^{N_c} C_k(\gamma_k) \right) \quad (3.8)$$

This method is commonly termed capacity effective SNR mapping (CESM) and constitutes an already well-known mapping metric quite investigated in literature [17]. The estimation error, calculated as in (3.5), is around 1% and 5%, evaluated over many realizations for various MCS and n_B . Though the approach is reasonable only with the previous hypothesis on the OFDM bandwidth, the CSM shows quite good performances in terms of accuracy, in many doubly-selective scenarios as shown in Figures 3.4(a) and 3.4(b), Nevertheless, we have to observe that the estimate

performances have a quite strong dependence from the particular realization and that, in any case, the CESM gives an underestimate.

Exponential effective SNR mapping (EESM) Recently, a considerable attention was paid to the exponential effective SNR mapping (EESM). This method is derived from Chernoff Union Bound of the pairwise error probability (PEP) [18]. The basic idea is to find an equivalent SNR in the AWGN channel that corresponds to the same WER, using the Union-Chernoff bound to relate the error probability to the corresponding SNR in a subchannel, supposing it has an approximately constant channel response. This approach leads to the mapping formula

$$\gamma_{eff} = -\ln\left(\frac{1}{N_c} \sum_{k=1}^{N_c} e^{-\gamma_k}\right) \quad (3.9)$$

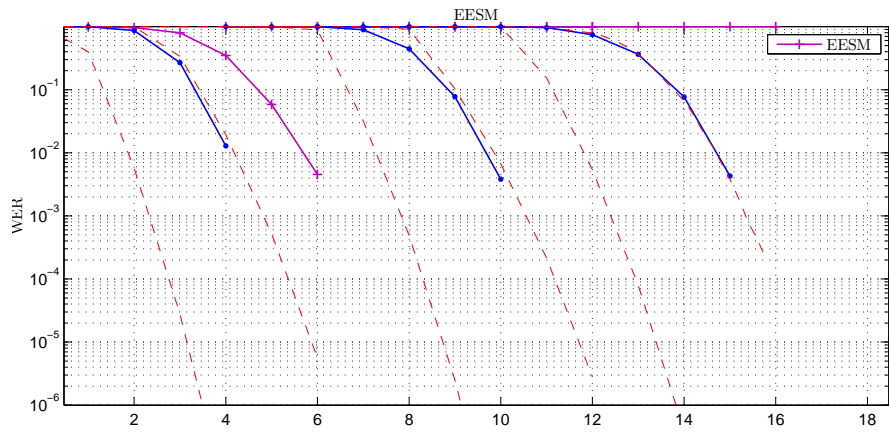
where we have used $I(x) = e^{-x}$.

The typical resulting estimate is usually much more pessimistic than the real WER, as for example in Figure 3.5, and this justifies the usage of a heavy scaling factor that can even assume the value of some dozens depending on the MCS [19]. Still in [18] it is shown that exponential ESM has a consistent accuracy if used as an ESM function for convolutional codes. For this reason, we can state that in our evaluation hypothesis, without using any scaling factor and with a duo-binary turbo coder, the EESM doesn't perform well.

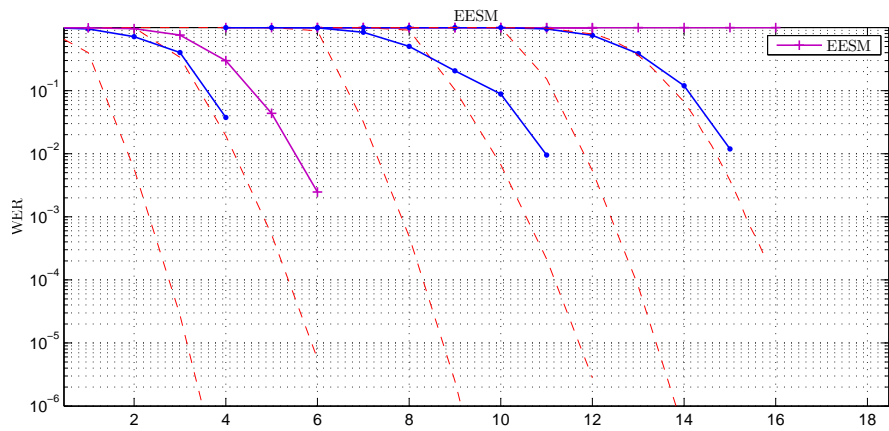
Logarithmic effective SNR mapping (LESM) Another possible mapping function is constituted by the logarithmic ESM, where precisely the function $I(\cdot)$ is a base ten logarithm:

$$\gamma_{eff} = 10^{\frac{1}{N_c} \sum_{k=1}^{N_c} \log_{10}(\gamma_k)} \quad (3.10)$$

As shown in Figure 3.6 this metric gives estimate very close to the real WER trend with an estimate error ϵ always below 5%. Moreover, it provides an overestimate. This fact is very important in a link adaptation context where, supposing that we are not optimizing scaling parameters, we don't have sufficient accurate estimate with a desirable estimate error below 1%. In fact, when selecting the transmission resources, it is always better to use a margin for overdimensioning the system. However, we can start to notice in both Figures 3.6(a) and 3.6(b) that the estimate curve

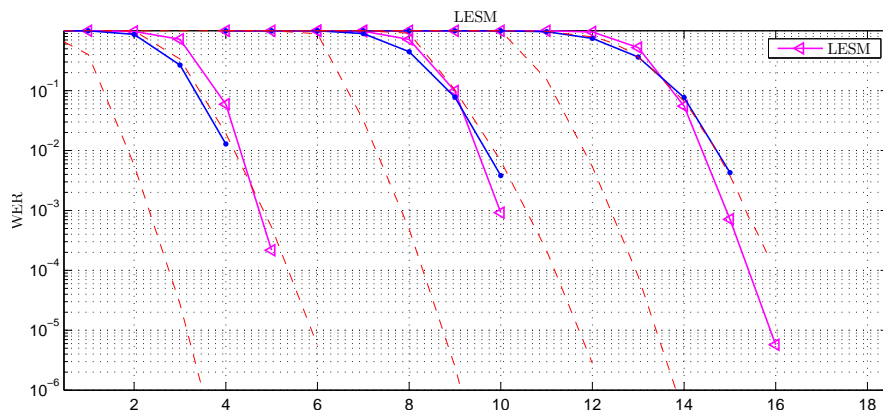


(a) $n_B = 1$

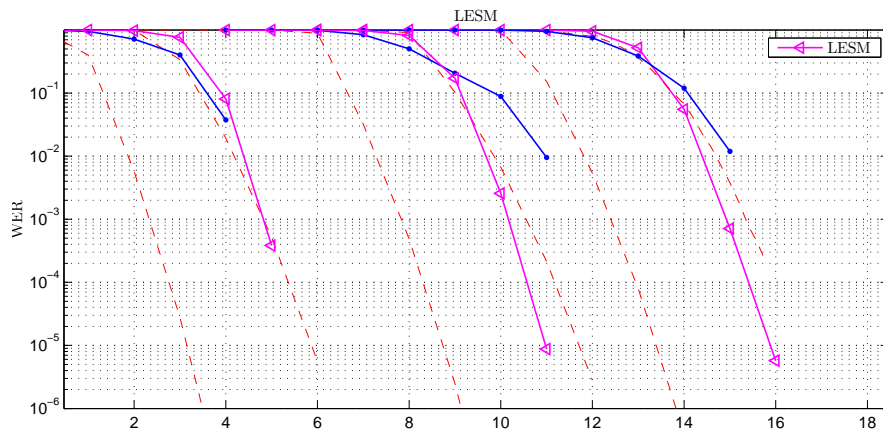


(b) $n_B = 4$

Figure 3.5: EESM performances for QPSK, 16QAM and 64QAM with $R_2 = 0.5$ and $n_B = 1, 4$. Dashed lines represent the AWGN and Rayleigh theoretical curves for each modulation



(a) $n_B = 1$



(b) $n_B = 4$

Figure 3.6: LESM performances for QPSK, 16QAM and 64QAM with $R_2 = 0.5$ and $n_B = 1, 4$. Dashed lines represent the AWGN and Rayleigh theoretical curves for each modulation

has a trend which tends to cross the real WER and this, as we will better explain in section 3.2.3, can be a defect.

3.2.1 Rayleigh channel hypothesis

As we discussed before, without any scaling factor it is quite difficult to have a reliable estimate of the WER in a doubly-selective channel. The only one method that seems to give a quite good accuracy is, in this context, the LESM.

Anyway we can make some observations:

- The CESM offers in any case an underestimate of the real trend of the WER
- The EESM, without any scaling factor, excessively overestimates the result
- The LESM method, though it shows good performances and a little overestimate, has a trend with a different slope from that of the simulated WER.

With our adaptation goal, if no accurate estimate is available, it would be fine to have an overestimate of the real WER with the same slope. This idea is acceptable only if we impose a trade-off between the system WER and the minimum throughput because, of course, we don't want to have a too worse evaluation of our transmission environment as this would lead to a waste of capacity.

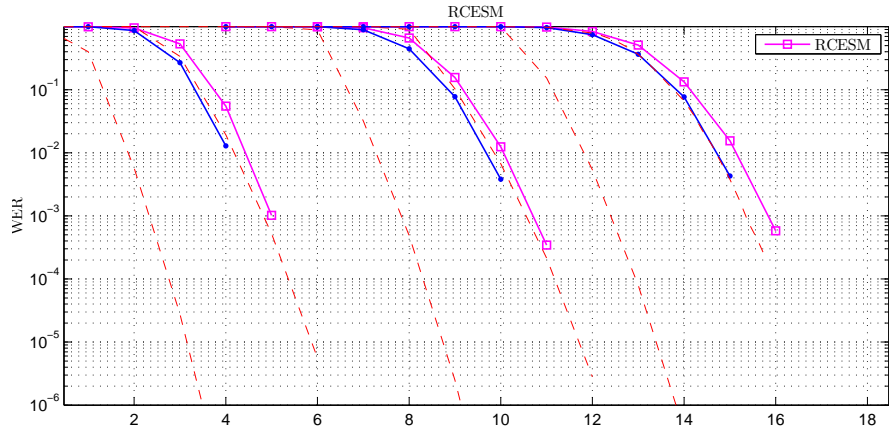
Aimed by this observation, we think about using the capacity approach with a worse assumption: we choose the Rayleigh channel WER of (2.11) as reference curve. This leads to a variant of the CESM method that we call for this reason RCESM. In other words, instead of using the Gaussian capacity formula to average and map the instantaneous SNRs, we use the Rayleigh channel capacity formula. This is a non-closed formula which is given by

$$I(x) = \frac{1}{\ln 2} \cdot e^{\frac{1}{x}} \cdot E_1\left(\frac{1}{x}\right) \quad (3.11)$$

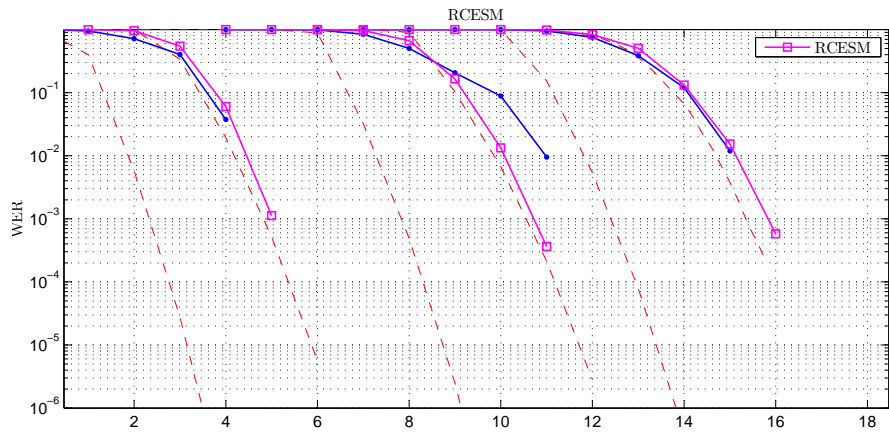
with

$$E_1(x) = \int_x^\infty \frac{e^{-t}}{t} dt \quad (3.12)$$

Simulation results in Figures 3.7 show that this metric provides an overestimate of the real WER, with the same slope, and with good accuracy. However we have to notice that the final result has a medium estimate error between 1% and 10% and therefore higher than LESM and CESM. This is due to a higher variance of the result, as the performance depends somehow from the particular realization.



(a) $n_B = 1$



(b) $n_B = 4$

Figure 3.7: RCESM performances for QPSK, 16QAM and 64QAM with $R_2 = 0.5$ and $n_B = 1, 4$. Dashed lines represent the AWGN and Rayleigh theoretical curves for each modulation

3.2.2 Other methods

Trying to obtain an alternative mapping method that sets aside ESM, we investigate the performances of a function different from (3.4). We propose a different method to map $\bar{\gamma}$ into γ_{eff} thinking about the weighted mean as a good kind of average which allows us to adjust the weights in relationship with the channel trend. Our mapping function is therefore

$$\gamma_{eff} = \frac{\sum_{k=1}^{N_c} w_k \gamma_k}{\sum_{k=1}^{N_c} w_k} \quad (3.13)$$

Now the question that rises is how to choose the weights w_k . Since the channel coefficients are Rayleigh distributed, the instantaneous SNRs γ_k are exponentially distributed with probability distribution function:

$$f_{\gamma_k}(x) = \frac{1}{\bar{\gamma}} e^{-\frac{x}{\bar{\gamma}}} \quad \text{for } x \geq 0 \quad (3.14)$$

whose trend is shown in Fig. 3.8.

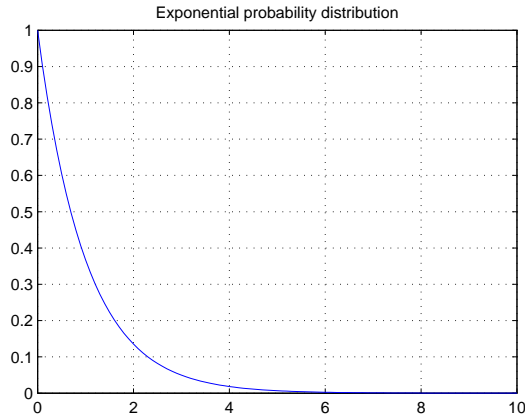


Figure 3.8: exponential distribution with $\bar{\gamma} = 1$

We quantize this function on a finite number of N_{bins} intervals in which we divide the range of the possible channel coefficients values. The idea is to exploit the channel information with a sort of probability distribution function weighted algorithm, defining:

$$p_j = f_{\gamma_k}(\gamma_j) \quad \text{for } j = 1, \dots, N_{bins} \quad (3.15)$$

Depending on the mapping hypothesis, we decide to which fading values give more weight, between the low or the high ones. We therefore have to distinguish between two cases: whether the look-up table, or the reference curve, is constructed for the Gaussian channel or for the Rayleigh channel.

Starting to analyze the second case, we immediately notice that, in this situation, we have to estimate a WER curve that is generally lower than the reference curve, which often happens when referring to the Rayleigh fading. This situation corresponds to the example shown in Fig. 3.3. To have the same trend of the simulated curve, the estimated effective SNR γ_{eff} should be higher than the initial SNR, $\bar{\gamma}$. Noticing this particular, it's reasonable to give more weight to higher channel coefficients which are, as we can see from the probability distribution function, the least probable. But if referring to the cumulative distribution function which, as we know is:

$$\begin{aligned} F_{\gamma_k}(\gamma_j) &= Pr\{\gamma_k < \gamma_j\} \\ &= \int_{-\infty}^{\gamma_j} f_{\gamma_k} d\gamma_k \\ &= \sum_{n=1}^j p_n \end{aligned} \tag{3.16}$$

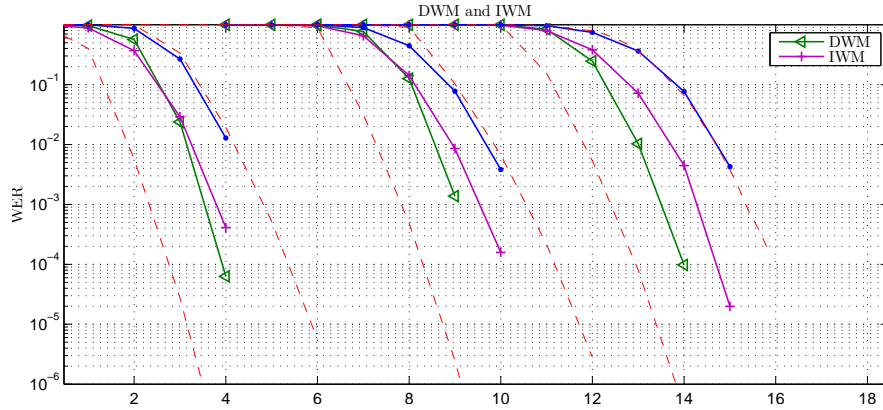
those coefficients acquire high values. We then choose for this situation a w_k which is proportional to the cumulative probability of the channel coefficients values. In particular, if the value of the instantaneous SNR γ_k corresponds to the j -th bin, we choose:

$$w_k = \sum_{n=1}^j p_n \tag{3.17}$$

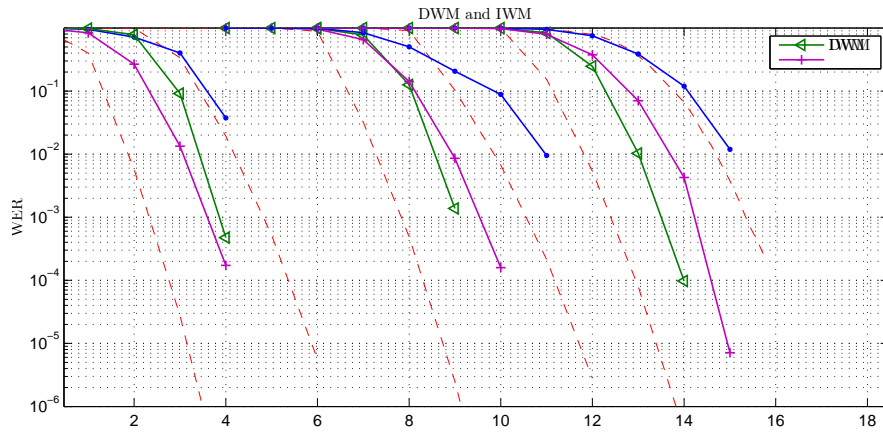
As the overall average γ_{eff} will result higher than the initial SNR value $\bar{\gamma}$ we call this method increased weighted mean or IWM. Simulations results as in Fig. 3.9 show that, estimating the WER with such a method has performances similar to the CESM when the real WER is near and below the Rayleigh fading curve. We therefore classify IWM as a reliable alternative to the ESM based mapping.

For the other case, when we base our mapping on the AWGN reference curve, we should follow the same criteria and therefore choose weights inversely proportional to the cumulative distribution function:

$$w_k = \frac{1}{\sum_{n=1}^j p_n} \tag{3.18}$$



(a) $n_B = 1$



(b) $n_B = 4$

Figure 3.9: DWM and IWM performances for QPSK, 16QAM and 64QAM with $R_2 = 0.5$ and $n_B = 1, 4$. Dashed lines represent the AWGN and Rayleigh theoretical curves for each modulation

so that the global metric would be penalized by the lower values of the channel. We therefore speak of decreased weighted mean or DWM. Simulations results still in Figure 3.9 show that this method has good performances in many cases, when we are closer to the AWGN channel performances, but still inferior to that ones of CESM metric.

For this reason we don't go into this method more than this brief description.

3.2.3 Performances

In this section, the subset of investigated link performance models is evaluated in terms of WER prediction accuracy. To have a performance evaluation of each ESM method, we have to compare the estimated \widehat{WER} with the WER derived from the simulations.

As we mentioned before, the validation procedure of each method is an off-line test. In fact, when checking the estimate performances, we don't simulate a realistic transmission, with a real channel model as described in chapter 2.5. In this section we state more precisely the problem to better understand the evaluation methodology .

The link adaptation procedure bases itself on the channel coefficients that affect the first OFDM symbol of each frame and then applies the selected MCS to all the following symbols, until a new frame starts. This means that we need to have a reliable estimate of the *instantaneous* WER evaluated on the duration of an OFDM symbol. It is now more clear why the evaluation method has to be an off-line process where the channel realization for one OFDM symbol is repeated over a certain number of symbols, to finally calculate the estimate WER and compare it with the simulated one. All the previous figures were obtained with this method.

However, the resulting instantaneous WER is quite random and therefore it is difficult to have a general evaluation of the method in this way. To obtain a global result, we plot the couples $(\gamma_{eff}, WER(\bar{\gamma}))$ and compare them with the used reference curve.

Considering a certain reference curve, that will be depicted in the following figures as a solid line, the match between this curve and the points relative to each estimate reveals the accuracy of the method. In fact, if we have perfect estimate, then the plotted curve corresponds to the reference one perfectly, otherwise there will be a certain shift or dispersion of the estimate points. Note that, in this representation,

the points that are underneath the reference curve corresponds to an overestimate while the points that stays above comes from an underestimate curve.

After having explained this validation procedure, we present a set of results in which are shown the estimate performances of each method, for $n_B = 1, 4$ for QPSK, 16QAM and 64QAM modulations with coderate $R_2 = \frac{1}{2}$.

CESM In Figure 3.10 are shown the performances of the CESM method for a channel model with $n_B = 1$ and $n_B = 4$ over a QPSK, a 16QAM and a 64QAM with $R_2 = \frac{1}{2}$.

The desirable thing is to have a set of points matching the reference curve with a low dispersion. We remember that, plotting $(\gamma_{eff}, WER(\bar{\gamma}))$, the used reference curve acts like a mirror for the mapped points and this means that, if $\widehat{WER}(\bar{\gamma})$ was underneath [above] the simulated $WER(\bar{\gamma})$, now the points that stay above [underneath] the reference curve. Given this, we can start to comment the ESM results.

Using the Gaussian capacity as the ESM function has the advantage of being a simple method though, as we said, is constrained by the Gaussian hypothesis itself. In fact the \widehat{WER} stays always underneath the real trend and this can be a problem when adapting under a certain WER constraint. In Figures 3.10(a), 3.10(c) and 3.10(e), where $n_B = 1$, we can see that the mapped points draw a curve with a certain bias: the average of those points, for each SNR, gives rise to a WER value which is different from the reference curve. Thus, the CESM result is, speaking as in estimate theory, incorrect, as it doesn't converge to the desired curve. Anyway, we can appreciate that it has a small variance and so also small granularity.

Comparing the three figures we then notice that for higher modulation orders the bias, and therefore the deviation from the reference curve, decreases and for 64QAM the result is quite close to the AWGN curve, though it still corresponds to an underestimate of the simulated WER. On the contrary, the granularity gets worse, as for 16QAM and 64QAM the points appear more scattered and this represent, in our estimate context, a defect. This tendency of the granularity, which gets worse for higher modulations, can be noticed also in Figures 3.10(b), 3.10(d) and 3.10(f) but here the result is even worse than the others: also increasing the number of correlated subcarriers, n_B , the estimate results become very scattered. This can be explained referring to the extreme case of Figure 2.6, where the WER tends to get very high increasing n_B and so is more difficult to chase accurately.

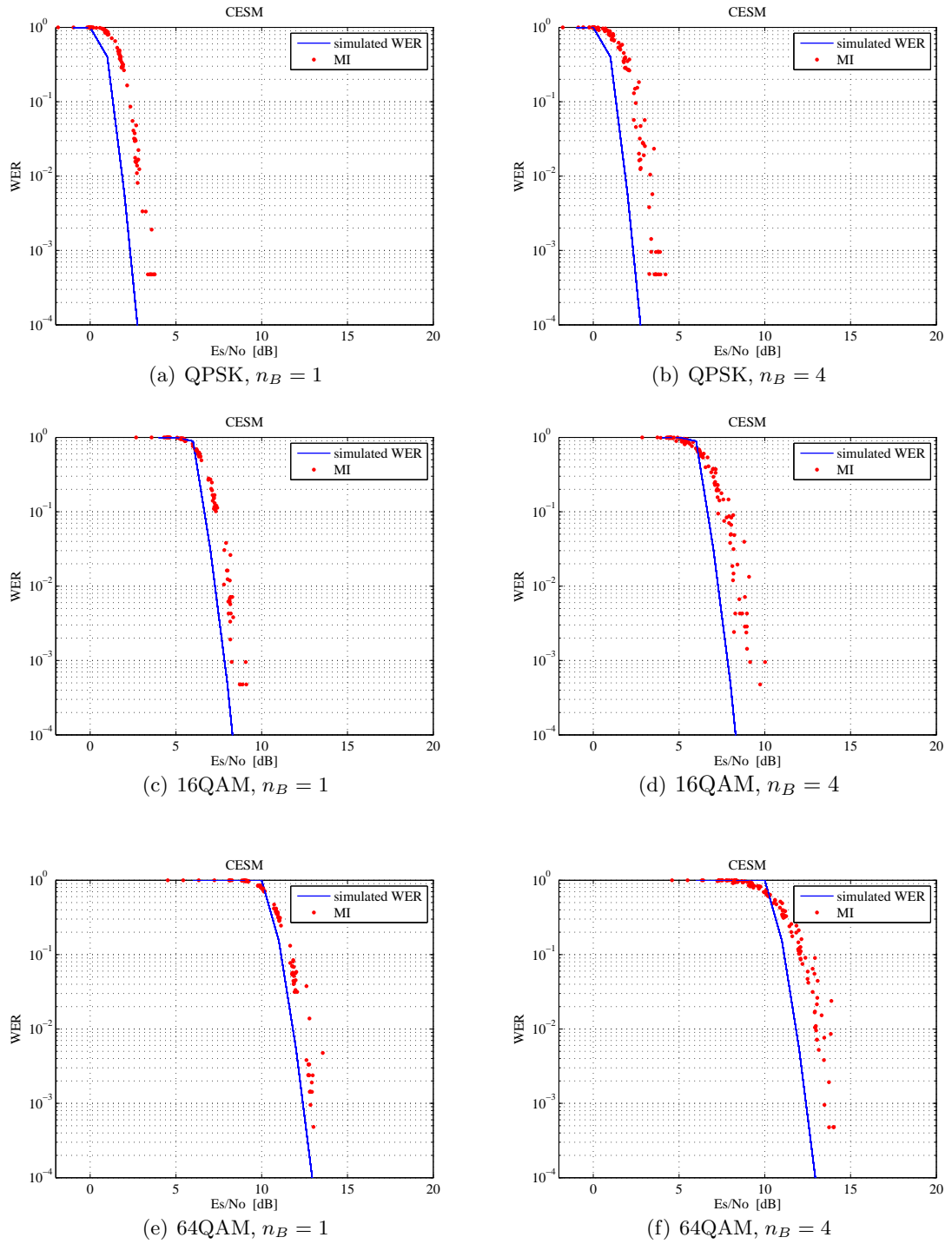


Figure 3.10: Performances of CESM method over QPSK on channel model with $n_B = 1$ 3.10(a), $n_B = 4$ 3.10(b); 16QAM with $n_B = 1$ 3.10(c), $n_B = 4$ 3.10(d); 64QAM with $n_B = 1$ 3.10(e), $n_B = 4$ 3.10(f). $R_2 = \frac{1}{2}$

EESM The EESM is a promising method, thanks to its good correlation among the estimate results, but without any scaling factor, performs quite bad. This is what emerges from the analysis of Figure 3.11, where the estimate results of the same previous cases are depicted.

In Figures 3.11(a), 3.11(c) and 3.11(e) in fact the mapped points draw clearly a specific curve, denoting a strong correlation among the estimates. Nevertheless, we clearly see that the results are strongly affected by a bias, that induces the envelop curve to deviate from the reference curve. This bias is heavier for higher modulation orders as it gives rise to a gap that goes from 1 dB for the QPSK, which is not so bad as in Figure 3.11(a), to 8 dB in the worst case of the 64QAM, shown in Figure 3.11(e).

The same considerations are valid also for Figures 3.11(b), 3.11(d) and 3.11(f) with $n_B = 4$, with the difference that here the mapped points present more scattering, as for the CESM method.

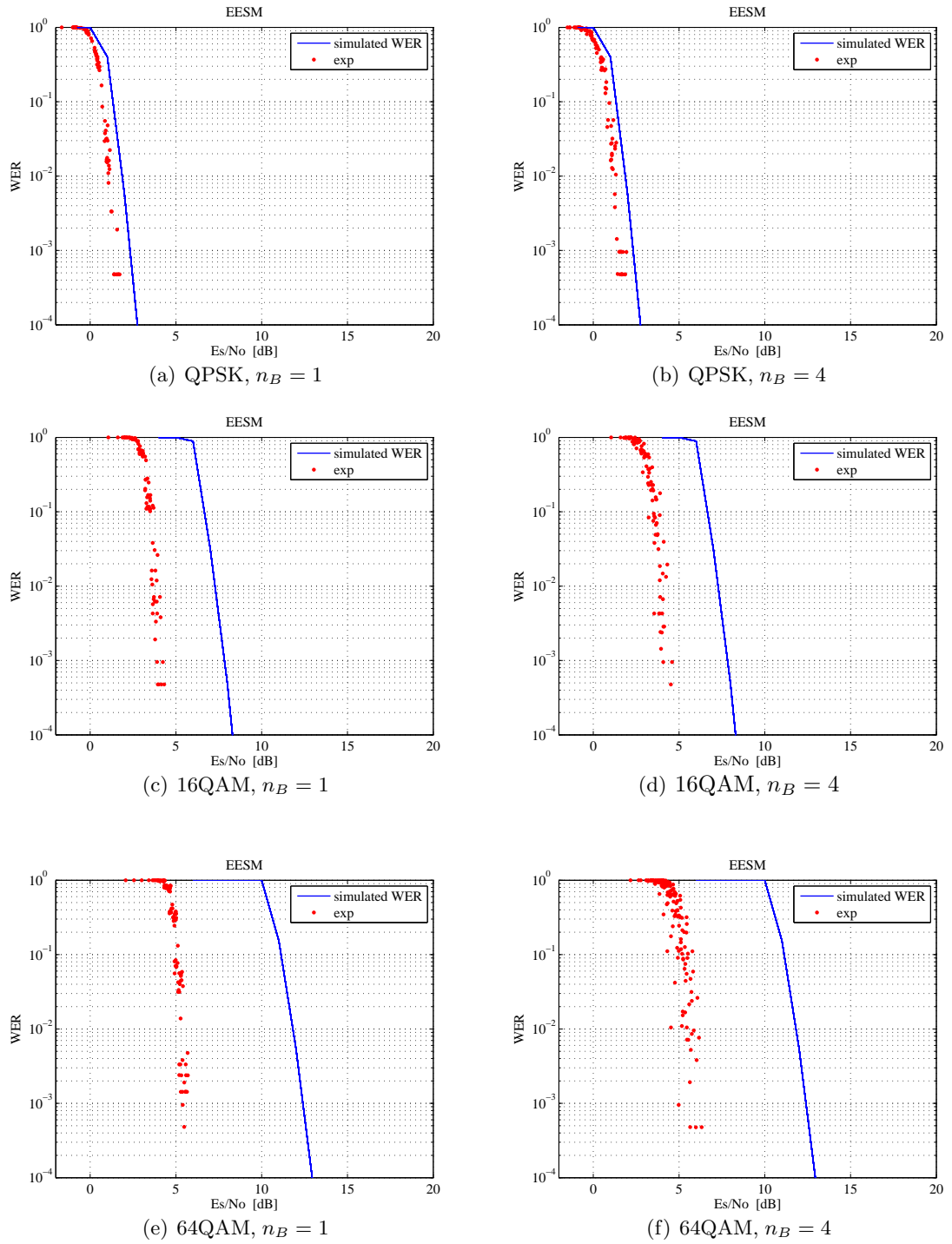


Figure 3.11: Performances of EESM method over QPSK on channel model with $n_B = 1$ 3.11(a), $n_B = 4$ 3.11(b); 16QAM with $n_B = 1$ 3.11(c), $n_B = 4$ 3.11(d); 64QAM with $n_B = 1$ 3.11(e), $n_B = 4$ 3.11(f). $R_2 = \frac{1}{2}$

LESM As forecasted in Figure 3.6, logarithmic effective SNR mapping performs quite well. Except from Figures 3.12(d) and 3.12(f), where there is too much scattering for individuating an envelop, the mapped points of each estimate are very close to the reference AWGN curve. This fact corresponds to a quite accurate estimate of the simulated WER and, unlike the other methods, the LESM preserves this property for all the modulation orders.

The mapping method presents therefore a quite good match with the reference curve and also a low variance of the estimate, as the points collapse on a specific path: looking at these results, this method can be apparently classified as a good link performance model.

Nevertheless, this path has clearly a trend that tends to cross the solid curve, as we noticed also in Figure 3.6. The mapped points are underneath the AWGN curve for low SNRs and then cross it in an intercept point that is higher for increasing modulation order: if for QPSK it is below $WER = 10^{-3}$, for 16QAM and 64QAM (in Figures 3.12(c) and 3.12(d)) it is above $WER = 10^{-1}$. This fact leads to have an underestimate for medium-high SNRs for high MCS and therefore we expect to have some undesired picks of errors using LESM in the link adaptation results.

RCESM In addition to the consideration on the link performance models already present in literature, we have introduced an ESM method that is based on a different channel hypothesis. With the RCESM in fact our reference curve is the Rayleigh channel WER, given from (2.11), with the proper parameters for each MCS from Table 2.2. Thus, in Figure 3.13 are shown the performances of this method referring to that curve.

The result of the estimate presents a certain granularity but, speaking as in estimate theory, it is correct: for each SNR, the trend of the estimate matches quite accurately the reference curve and this corresponds to a negligible bias. In this trend we can observe also a tendency for an overestimate which is, as we said, more desirable than an underestimate. In particular, in Figure 3.13(e), the scattered points are all underneath the reference curve, with a maximum deviation of 1 dB.

From the comparison of Figure 3.13(a), 3.13(c), 3.13(e) and 3.13(b), 3.13(d), 3.13(f) we can see once more that increasing n_B results in a worse dispersion for all the MCS, but unlike LESM, where the deviation reaches even 2 dB, this scattering leads to smaller errors. Anyway we can expect that, in these cases, the underestimate of the WER will probably cause the selection of inappropriate MCS when adapting. Taking into account all these details, we think of using RCESM method in a system

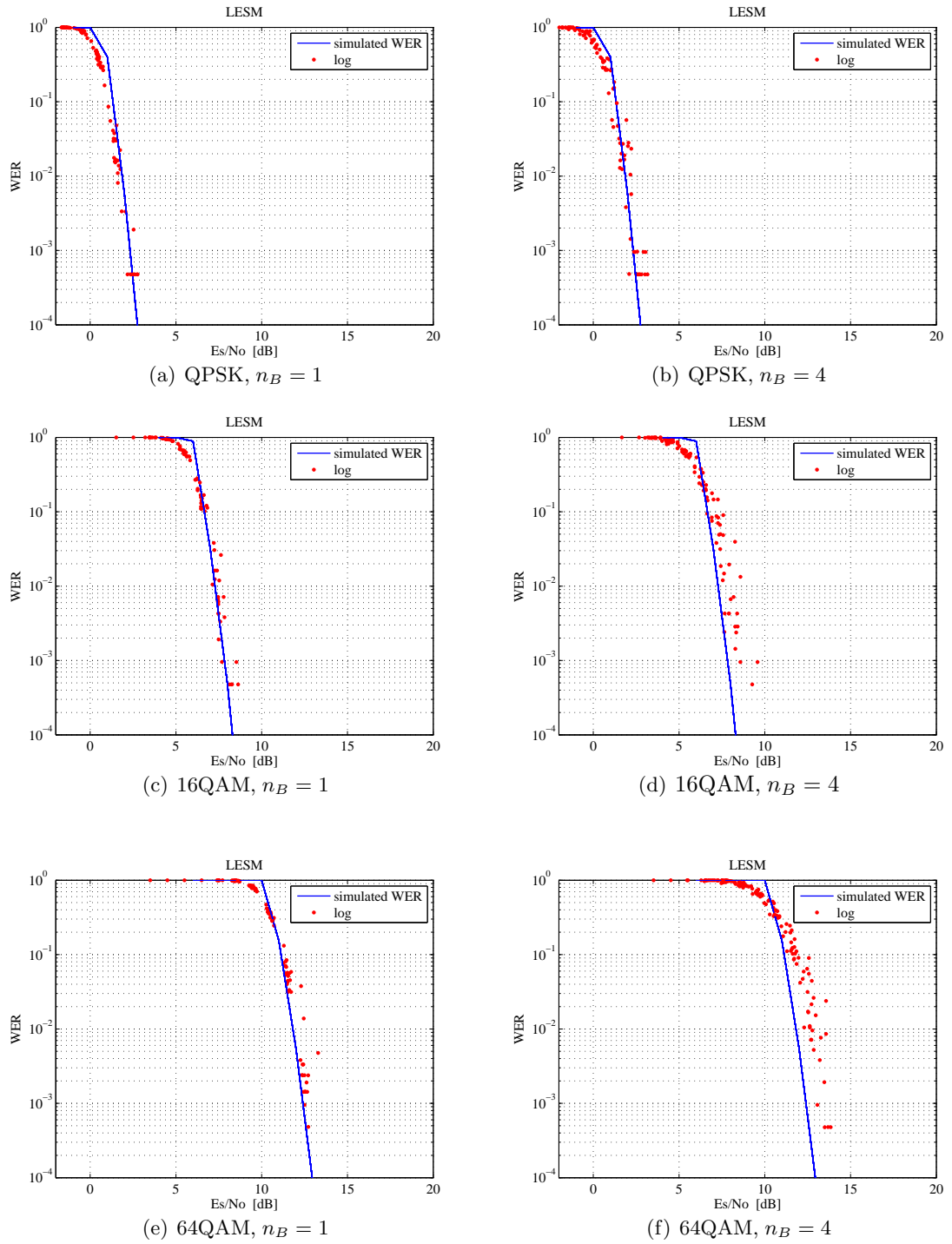
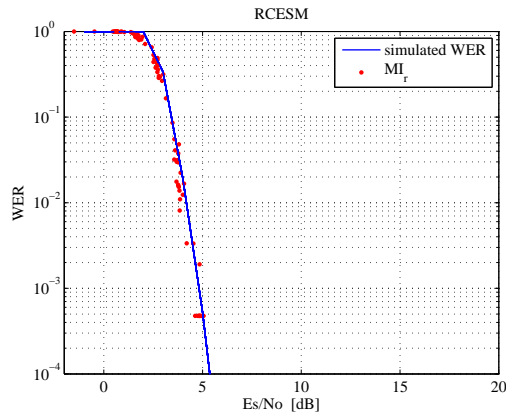
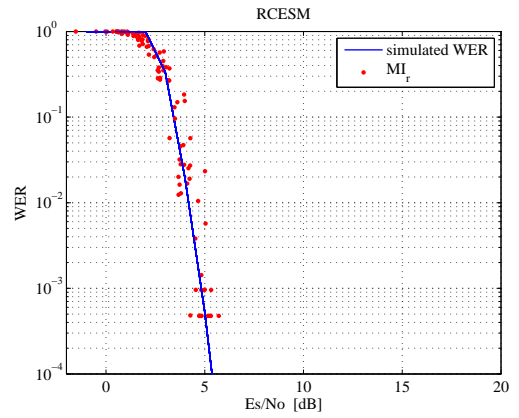


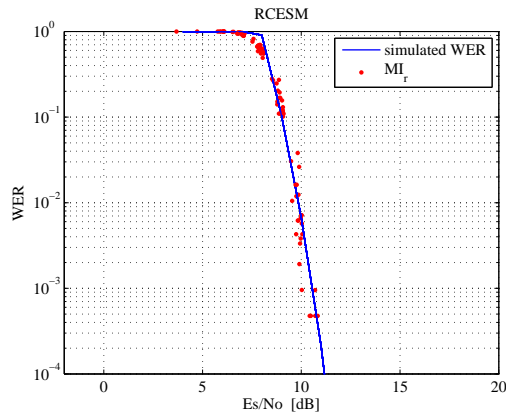
Figure 3.12: Performances of LESM method over QPSK on channel model with $n_B = 1$ 3.12(a), $n_B = 4$ 3.12(b); 16QAM with $n_B = 1$ 3.12(c), $n_B = 4$ 3.12(d); 64QAM with $n_B = 1$ 3.12(e), $n_B = 4$ 3.12(f). $R_2 = \frac{1}{2}$



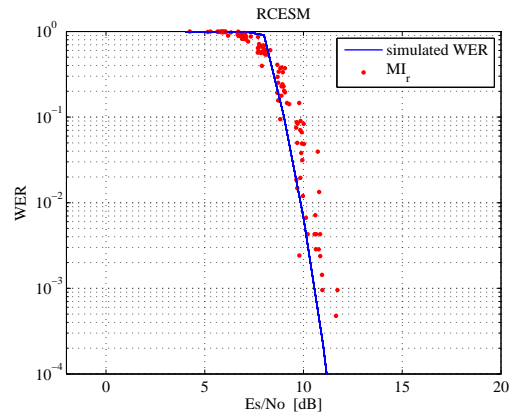
(a) QPSK, $n_B = 1$



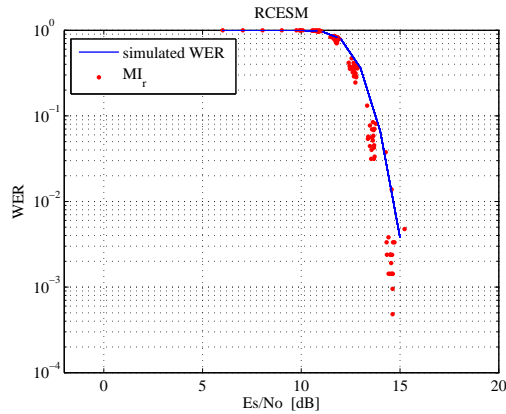
(b) QPSK, $n_B = 4$



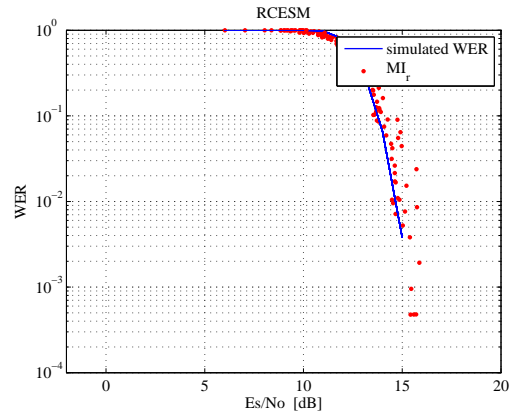
(c) 16QAM, $n_B = 1$



(d) 16QAM, $n_B = 4$



(e) 64QAM, $n_B = 1$



(f) 64QAM, $n_B = 4$

Figure 3.13: Performances of RCESM method over QPSK on channel model with $n_B = 1$ 3.13(a), $n_B = 4$ 3.13(b); 16QAM with $n_B = 1$ 3.13(c), $n_B = 4$ 3.13(d); 64QAM with $n_B = 1$ 3.13(e), $n_B = 4$ 3.13(f). $R_2 = \frac{1}{2}$

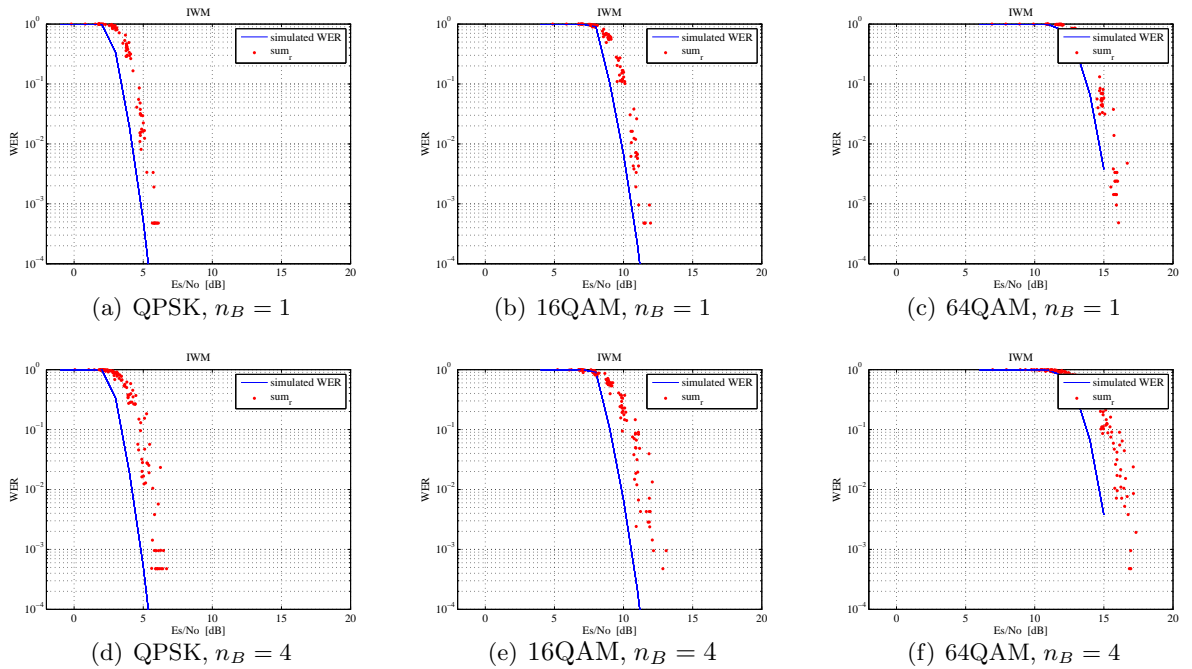


Figure 3.14: Performances of IWM method over QPSK on channel model with $n_B = 1$ 3.14(a), $n_B = 4$ 3.14(d); 16QAM with $n_B = 1$ 3.14(b), $n_B = 4$ 3.14(e); 64QAM with $n_B = 1$ 3.14(c), $n_B = 4$ 3.14(f). $R_2 = \frac{1}{2}$

where it is included also a frequency interleaver that guarantees the channel characteristic of $n_B = 1$. In this way we are sure to have a quite accurate estimate using CESM without the need of any scaling factor.

Looking at the global performance, it is therefore interesting to consider RCESM as a possible link performance model.

IWM and DWM The presented algorithms were all based on ESM approach. In section 3.2.2 we introduced two possible algorithms based on the weighted mean. Looking at Figure 3.9 we could already do some comments on the expected performances: in 3.9(a) the IWM estimate had an accuracy similar to that one of CESM, while DWM showed its inefficiency; then, the curves depicted in 3.9(b) were both very distant from the simulated WER.

In Figures 3.14 and 3.15 are shown the mapped points of each estimate WER, for

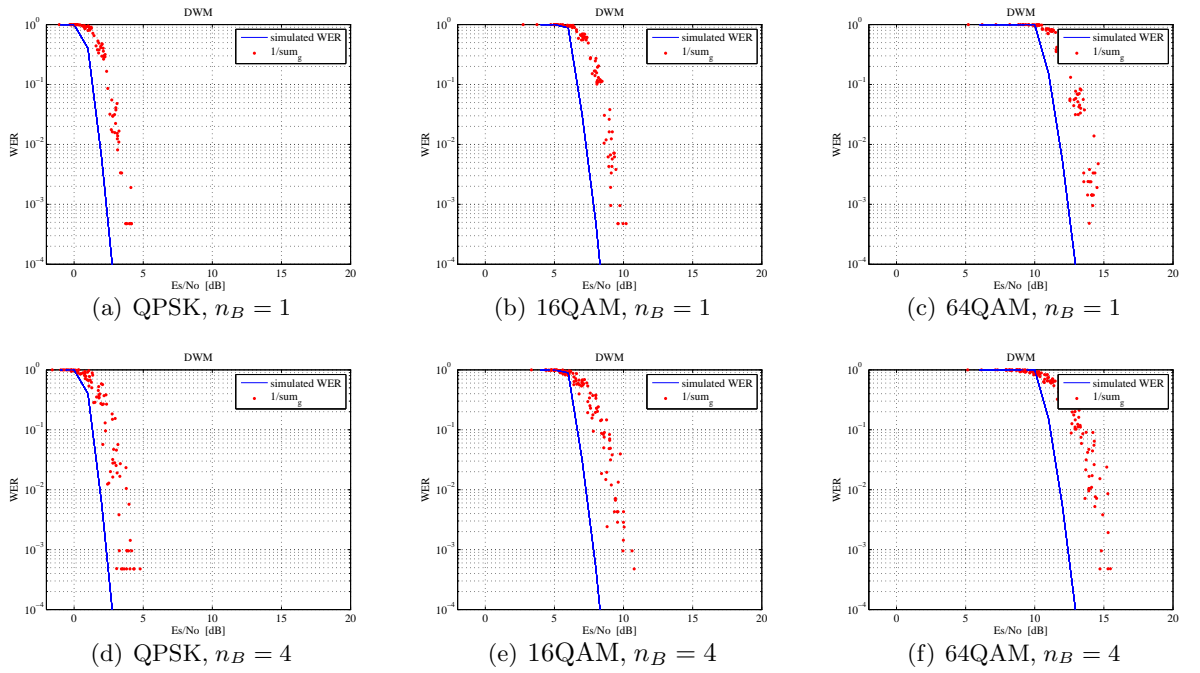


Figure 3.15: Performances of DWM method over QPSK on channel model with $n_B = 1$ 3.15(a), $n_B = 4$ 3.15(d); 16QAM with $n_B = 1$ 3.15(b), $n_B = 4$ 3.15(e); 64QAM with $n_B = 1$ 3.15(c), $n_B = 4$ 3.15(f). $R_2 = \frac{1}{2}$

many realizations to have a global evaluation. As expected, the two methods are not only incorrect, as they have a considerable deviation, but they appear also very scattered. Moreover, the points are always above each reference curve and this means that we have in every case an underestimate that can therefore induce undesired WER peaks. In conclusion we can state that the proposed weighted algorithms, based on the cumulative distribution function of the instantaneous SNRs, are not suitable for our link adaptation goal.

Chapter 4

Link Adaptation and HARQ

Link adaptation and hybrid automatic repeat request are two link level techniques proposed to increase throughput in wireless networks. LA dynamically adjusts the modulation and coding format based on an estimate of the channel condition, that is the WER estimate. HARQ performs the retransmission whenever the receiver cannot decode correctly a codeword.

4.1 Link Adaptation

In [13] was shown that the performance of every coding scheme strongly depends on the channel quality conditions, so if a fixed coding scheme is selected, the variation of the channel conditions during the transmission would lead to a performance loss. The aim of link adaptation is then to update the coding scheme according to the channel quality variations.

Supposing to have perfect channel estimate, the receiver can select the transmission scheme aware of the channel characteristics and send it through a feed back channel to the transmitter. Transmissions that do not use adaptive methods require a considerable link margin to guarantee acceptable performances when the channel state is bad. Therefore, the link budget of these systems is designed for the worst-case channel conditions, with a consequently inefficient utilization of the channel capacity. On the contrary, link adaptation allows the transmitter to perform an efficient transmission, exploiting favorable channel conditions and avoiding high rates in correspondence of deep fades [3]. Of course, if the channel is changing faster than it is estimated and feed back to the transmitter, the performances of this technique will be unsatisfactory.

4.1.1 Adaptation algorithm

In our context, the adaptive techniques are used to satisfy the QoS requirements, providing high spectral efficiency by transmitting at high rates under favorable channel conditions, and reducing throughput as the channel degrades. This can be done by varying the constellation size and the coding rate for a fixed SNR E_b/N_0 .

Link adaptation is then a process of automatically adjusting the transmission parameters, so that optimal quality of the communication is achieved. In our context, as we said, optimal quality means maintaining the WER below a certain value of WER_{max} , while keeping the data throughput as high as possible. In order to decide which rate is optimal, the adaptation algorithm needs informations about the current link conditions, that we have termed channel state information (CSI).

For a given SNR, different MCS achieve different WER performance. If we index the set of MCS of Table 2.1 by $c = \{1, 2, 3, 4, 5, 6, 7\}$, at a given SNR $\bar{\gamma}$, the throughput of MCS c can be defined as the average number of information bits in correctly received codewords which is given by

$$\eta^{(c)}(\bar{\gamma}) = R_1^{(c)} R_2^{(c)} (1 - WER^{(c)}(\bar{\gamma})), \quad c = 1, \dots, 7 \quad (4.1)$$

where $R_1^{(c)}$ is the number of bits for QAM symbol and $R_2^{(c)}$ is the coderate of MCS c .

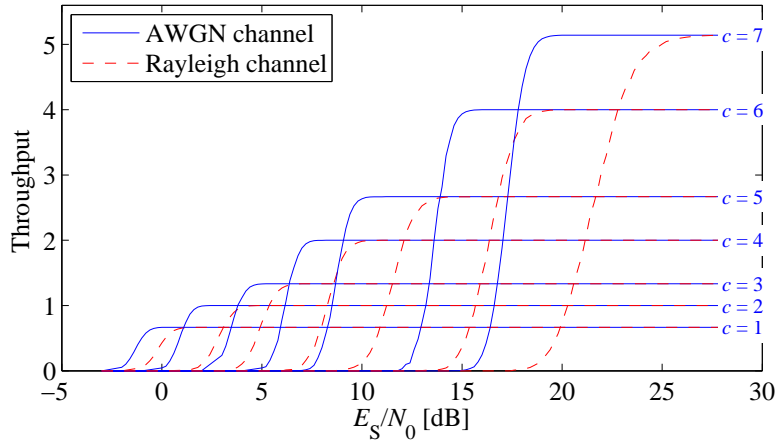


Figure 4.1: Throughput of the seven MCS over AWGN and Rayleigh fading channels

In Figure 4.1 it is shown the performance in terms of throughput for each modu-

lation and coding scheme available for the well known cases of AWGN and Rayleigh channel.

The adaptation algorithm applies the selected MCS for the whole duration of the frame, until a new frame starts and the algorithm adapts another time its transmission parameters. First of all, as we are neither working in an AWGN nor in a pure Rayleigh fading channel, we need to have the WER estimate. This estimate, that we indicate as $WER^{(c)}(\bar{\gamma})$, is relative to the particular channel realization on the first OFDM symbol of the frame and is a function of the mean SNR $\bar{\gamma}$, different for each MCS. Since we have imposed a WER constraint of $WER_{max} = 10^{-2}$, we can individuate a set of SNRs $\gamma_{req}^{(c)}$ that are chosen to have

$$WER^{(c)}(\gamma_{req}^{(c)}) = 10^{-2} \quad (4.2)$$

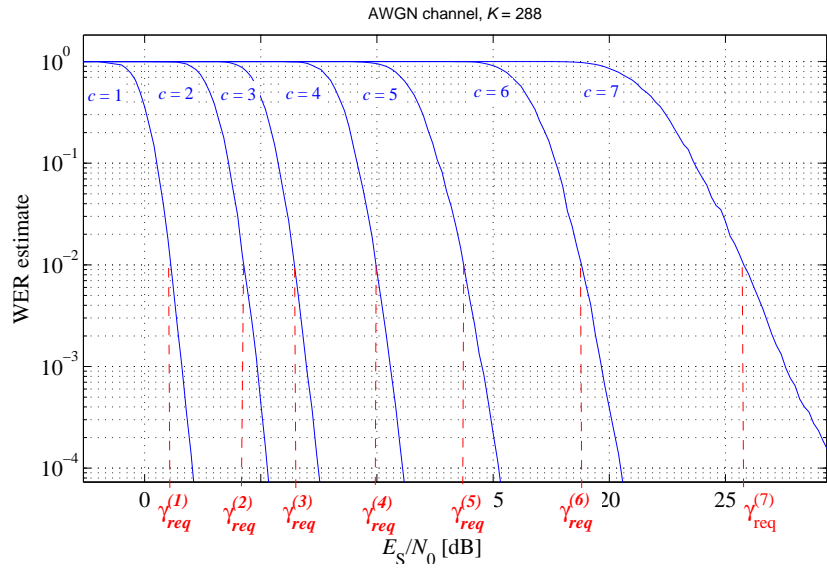


Figure 4.2: Link adaptation thresholds for the corresponding WER set of a Gaussian channel

as shown in Figure 4.2 still for the theoretical AWGN case. Once calculated this vector, the best MCS among $c = \{1, 2, 3, 4, 5, 6, 7\}$, for the particular channel realization, is selected as

$$c = \arg \max_c \{ \gamma_{req}^{(c)} < \bar{\gamma} \} \quad (4.3)$$

An alternative description of the adaptation algorithm can be also

$$c = \arg \max_c \left\{ WER^{(c)}(\bar{\gamma}) < WER_{target} \right\} \quad (4.4)$$

where, as we know, in our case $WER_{max} = 10^{-2}$. In some papers, the $WER^{(c)}(\bar{\gamma})$ is taken as the well known theoretical or analytical approximation for AWGN or Rayleigh fading channels [14], that we have indicated in (2.11). This solution represents a simplification of the problem because what we actually need is a WER estimate for the particular channel realization, as discussed in the previous chapter.

4.1.2 Link adaptation performances with various ESM criteria

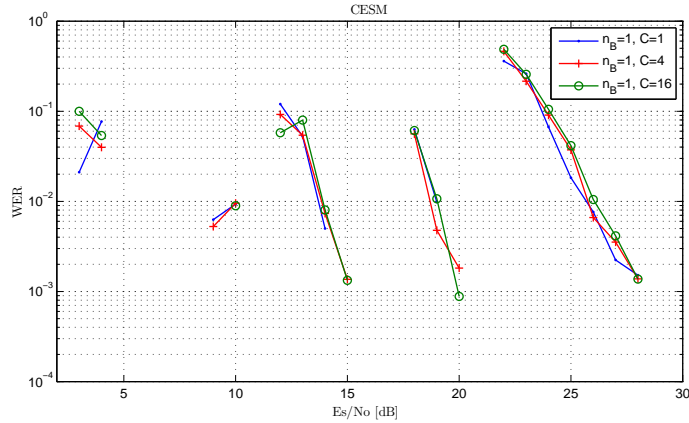
All the previous dissertation had the goal of calculating a WER estimate with a good accuracy, to further apply link adaptation on a meaningful scenario. This means that the final performances have to be evaluated looking at the adaptive coding and modulation (ACM) results, in terms of WER and throughput, basing each time our adaptation algorithm on one of the investigated ESM methods. Our goal is to obtain a WER that respects the constraint of 10^{-2} , maximizing at the same time the possible throughput. This means that we don't want to obtain a WER too much lower than the WER_{max} , as this would mean that we are keeping underneath the allowed throughput without maximizing it.

To obtain those results, we have to simulate a realistic transmission. We then generate a certain channel realization following the channel model described in section 2.5. In each simulation we characterize the transmission scenario in terms of number of correlated subcarriers n_B , on which the channel coefficient is constant, and number of OFDM symbols that experience the same channel realization, that is C . For a fixed SNR we have therefore a set of selected MCS, one for each frame of our transmission.

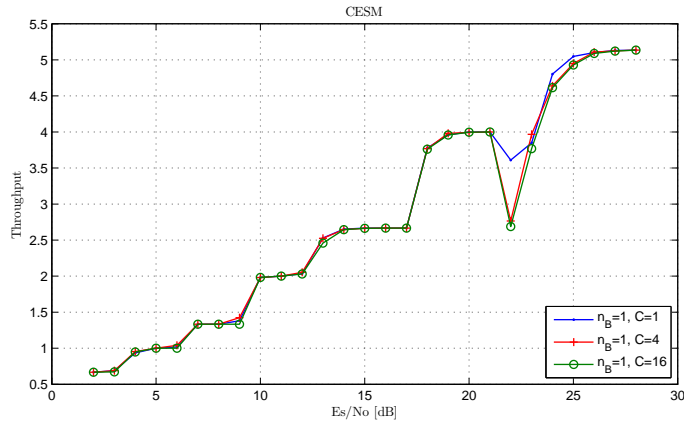
We can also view the link adaptation result for a certain frame, in terms of spectral efficiency and energy efficiency, just plotting the position of the selected MCS on the efficiencies plan. This result can be obtained simulating a pure AWGN channel with a WER constraint of $WER_{max} = 0$. As we are using a quite short codeword length of $K = 288$ we don't expect to see significant good performances, compared to the well known results of turbo codes that use longer codewords.

We list below the set of results obtained using each investigated ESM method for various channel models.

CESM As expected from the analysis of the CESM performances in Figures 3.10(a) and 3.10(b), with this estimate method we are not able to respect the WER constraint that we have imposed. This result could be already predicted noticing that the CESM estimate always gives rise to an underestimate of the real instantaneous WER.



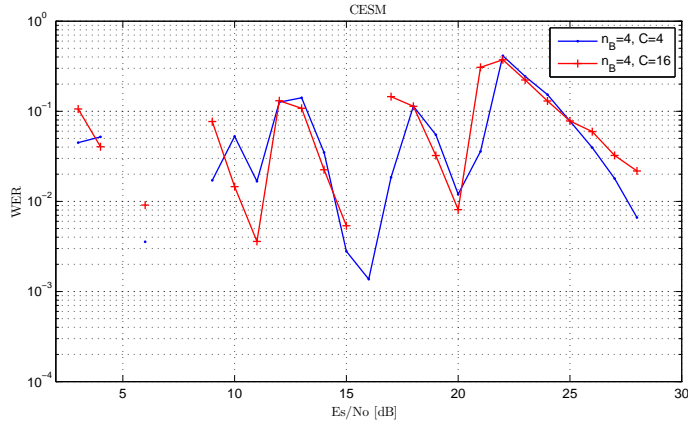
(a) WER



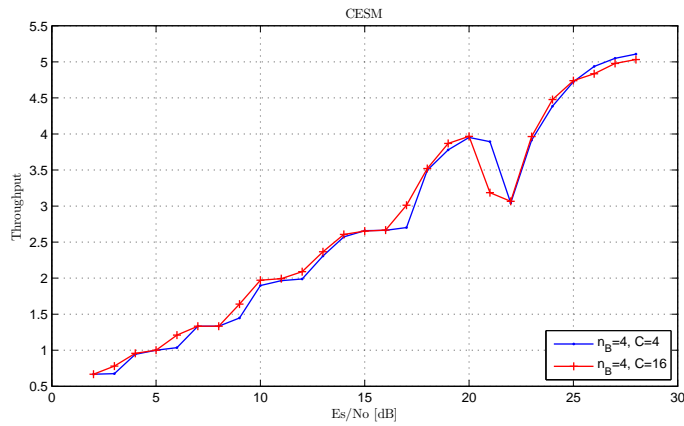
(b) Throughput

Figure 4.3: Link adaptation with CESM: resulting WER and throughput for $n_B = 1$ and different frame lengths

In Figures 4.3(a) and 4.3(b) are shown the results in terms of WER of the link adaptation on a selective channel with $n_B = 1$ and different frame length $C = \{1, 4, 16\}$ (the first case corresponds to a frame length equal to the OFDM symbol length). Comparing the results for different C we can state that this parameter



(a) WER



(b) Throughput

Figure 4.4: Link adaptation with CESM: resulting WER and throughput for $n_B = 4$ and different frame lengths

doesn't influence the result. This can be reasonable in a simulation scenario that doesn't take into account the channel estimate problem and its intrinsic delay. As we are supposing to have perfect channel state information, it's not important how frequently we have to adapt. Of course, in a real scenario, we expect to encounter significant adaptation problems if the channel is changing faster than it is estimated and feed back to the transmitter. Nevertheless, in our analysis we don't notice significant difference among the results of various C and therefore in the following we will expose only results calculated for a channel model with a frame of $C = 4$ OFDM symbols with the same channel realization.

Performances for a more correlated channel with $n_B = 4$ are shown in Figures 4.4(a)

and 4.4(b), where we still can see the effect of an inefficient MCS selection. We then complete the analysis of the CESM method showing in Figure 4.5 the points corresponding to the selected MCS for the first frame, in function of the average SNR E_b/N_0 , on the Shannon plane.

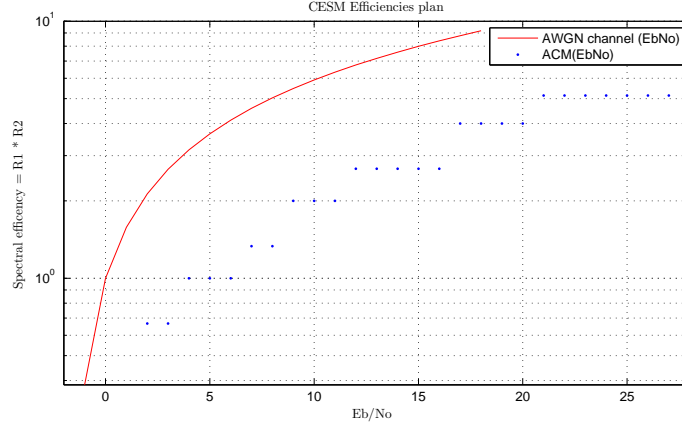


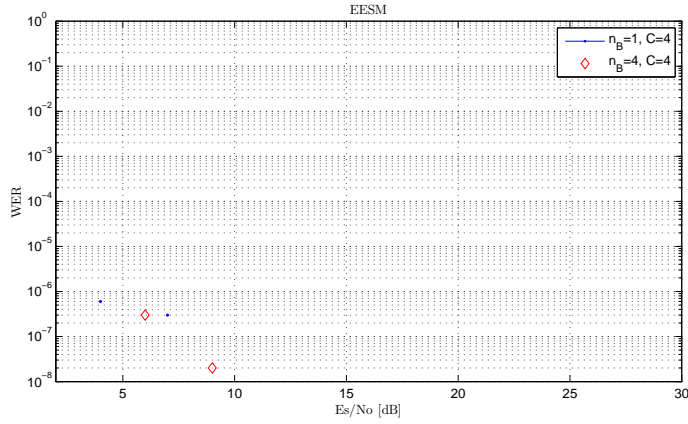
Figure 4.5: Efficiencies plan with link adaptation results using CESM on a AWGN channel

We can see the result of the ACM scheme, that jumps from one MCS to another depending on the SNR. The points of the selected MCS are not very close to the Shannon limit, but this could be expected as we are using a very short codeword length of $K = 288$.

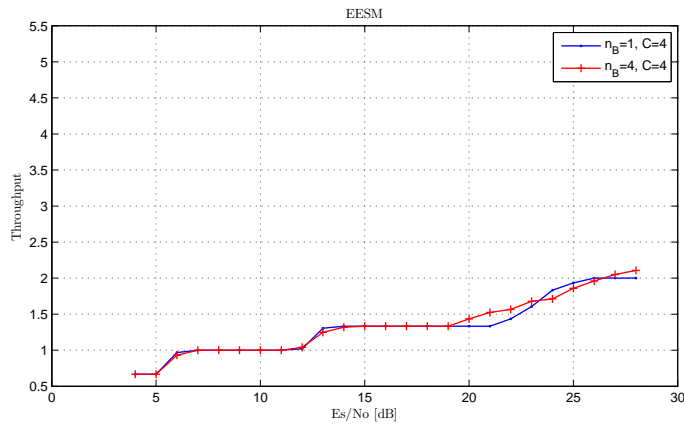
EESM In the previous chapter we saw that the EESM method, without any scaling factor, results in an exaggerated overestimate of the real WER. This fact ensures that the imposed WER constraint is respected, as we can see from Figure 4.6(a) where the resulting WER is even below 10^{-6} and 10^{-7} . Nevertheless, in Figure 4.6(b) we can clearly see the disadvantage of this method: the throughput is extremely low and therefore unacceptable.

We then conclude the analysis of the EESM stating that it can be a promising method as the resulting estimate has low dispersion and the same slope of the real WER, but with the condition of using a heavy correcting factor which is a crucial element for its performances.

LESM Though the result of the estimates in Figure 3.12 had a quite good match with the reference curve, also the LESM performs quite bad when applying link



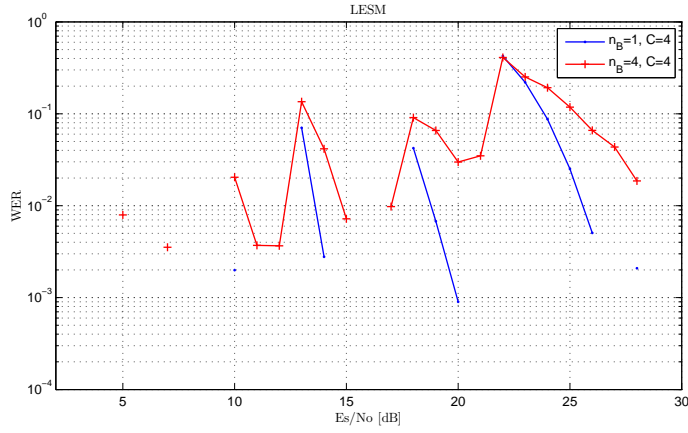
(a) WER



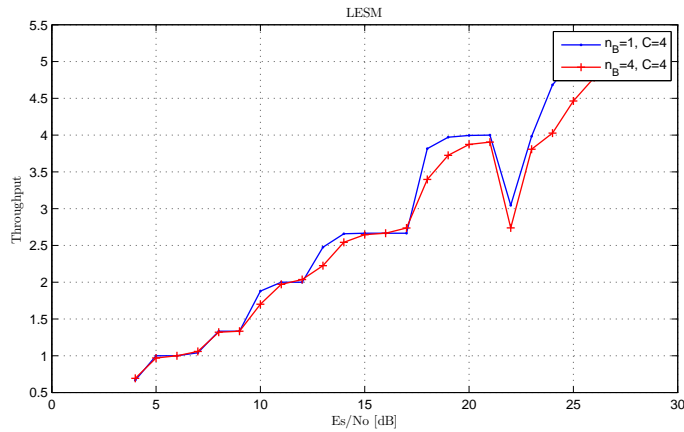
(b) Throughput

Figure 4.6: Link adaptation with EESM: resulting WER and throughput for $n_B = 1$, $n_B = 4$ and frame length of $C = 4$

adaptation as it doesn't respect the WER constraint of 10^{-2} . This can be seen in Figure 4.7 where, for both channel models, the resulting WER has many undesired picks. This can be explained observing that for an SNR of 13 dB, the selected MCS is one of the higher order, for example MCS 5, 6, 7. In Figure 3.12(c) we could see that, for increasing modulation order, the different slope of the LESM results led to a cross of the reference curve, resulting in a shift from an overestimate to an underestimate of the real WER. In fact, when the adaptation algorithm chooses higher MCS, as for SNRs from 13 dB and over, the final result doesn't respect the required condition.



(a) WER

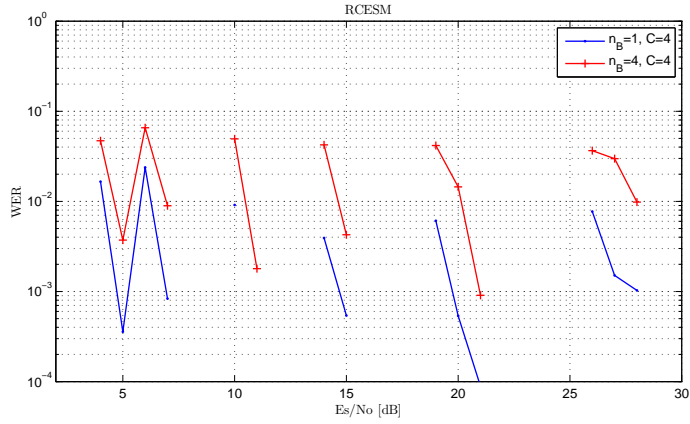


(b) Throughput

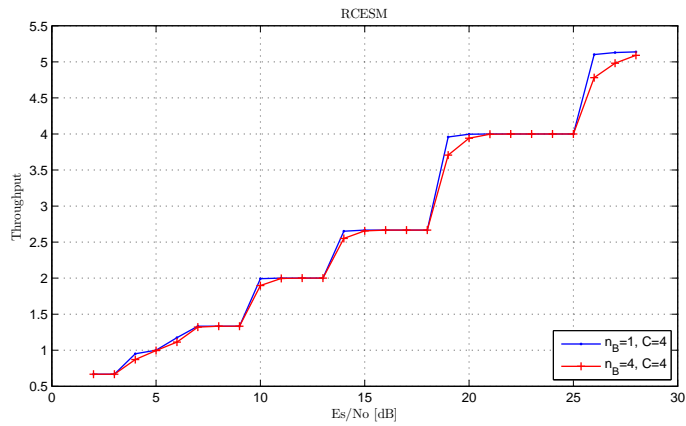
Figure 4.7: Link adaptation with LESM: resulting WER and throughput for $n_B = 1$, $n_B = 4$ and frame length of $C = 4$

RCESM In Figures 4.8(a) and 4.8(b) are shown the performances of a transmission using RCESM estimate algorithm for $n_B = 1$ and $n_B = 4$ respectively. It is interesting to see that for the case where $n_B = 1$ the RCESM shows the *best performances* among the evaluated methods. In fact, the WER constraint is nearly completely fulfilled and, at the same time, we reach a higher throughput compared to other method's result, without any fade.

In paragraph 3.2.3 we mentioned that it would be fine to include a frequency interleaver in the transmission system to obtain a perfectly interleaved channel. In fact those results suggest that, to have good performances of link adaptation without



(a) WER



(b) Throughput

Figure 4.8: Link adaptation with RCEM: resulting WER and throughput for $n_B = 1$, $n_B = 4$ and frame length of $C = 4$

including optimal scaling parameters in the estimate algorithm, the RCEM is the best method if used in a perfectly interleaved channel, which has $n_B = 1$. Moreover, using two interleaving methods has the advantage of better exploiting the diversity gain inherent in the channel, not only in the time domain but also in the frequency domain [20]. Taking into account all these details, we can state that using RCEM method in a system where that includes also a frequency interleaver guarantees very good performances even without optimizing the ESM method with scaling parameters.

To complete the discussion on this proposed method, we show in Figure 4.9 its

performances in terms of efficiencies of the selected MCS. We have to pay attention to the assumption used to obtain this figure, as apparently the CESM is closer to the Shannon limit than the RCESM, but in reality this is an obvious consequence of the AWGN channel hypothesis, that of course fits better with the Gaussian capacity based algorithm.

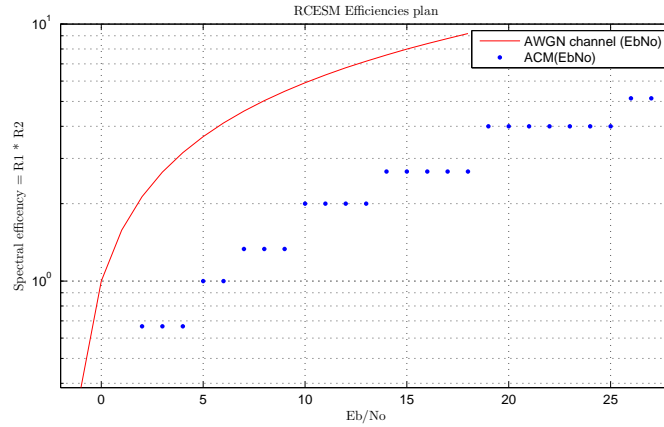


Figure 4.9: Efficiencies plan with link adaptation results using RCESM on a AWGN channel

4.2 Hybrid automatic repeat request (HARQ)

As we experienced in the link adaptation results, the WER estimate can constitute a significant constraint if it doesn't guarantee a good accuracy. In fact, in the cases where the applied ESM method didn't have a good match with the reference curve, the resulting WER was unacceptable. Moreover, if we consider the delay problem in a real scenario, caused by transmitting information on the feedback channel, the link adaptation performances can become strongly degradable if the channel is varying rapidly. Taking into account those problems, it is essential to include a retransmission mechanism that guarantees the correct reception of each packet: fast link-level retransmission can complement in this context the ACM strategy. As a feedback channel is available, it is possible to use an Automatic Repeat reQuest (ARQ) protocol in addition to the FEC schemes, where the receiver sends requests for the sender to repeat data unit transmissions whenever errors are detected. In particular, automatic repeat request (ARQ) retransmission is requested when error correction during decoding cannot correct all the errors in the received packet and, in this case, the receiver discards the incorrectly received codewords.

Another approach to error control uses the so called hybrid ARQ (HARQ) scheme that incorporates also FEC: the term Hybrid ARQ can be used to describe any combination of a FEC and ARQ schemes in which unsuccessful transmissions are used in FEC decoding instead of being discarded. If appropriate ARQ and FEC schemes are properly combined, hybrid ARQ can significantly increase the system performances.

A hybrid ARQ retransmission method in a communication system where data packets consists of modulation symbols encoded with a FEC scheme retransmits the incorrectly received codewords, or a part of them, basing on a repeat request. At the receiver side, the coded bits are later combined on the basis of the soft-information values and we can therefore state that it is applied a *soft combining* on the retransmitted information.

Given this, we illustrate the two possible HARQ schemes that are usually classified [21] as:

- HARQ Type I, termed Chase Combining (CC)

- HARQ Type II, termed Incremental Redundancy (IR)

Chase Combining Supposing to have an error in the decoding of a certain codeword \underline{c} , the *Chase combining* method consists in the simple repetition of the N bits $\underline{c} = [c_1, c_2 \dots, c_N]$ where we remember that $N = \frac{K}{R_2}$ as referring to Figure 2.2. This is the simplest way to perform HARQ, as each retransmission is an identical copy of the original transmission. In subsection 2.1 we spoke about a APP soft demapping performed at the receiver side. When applying Type I HARQ, the receiver simply adds the L-values of the retransmitted coded bits to the corresponding values of the previously received ones and then passes those values to the decoder. From a coding point of view we therefore speak of chase combining or *repetition coding*.

In our link adaptation context, we assume to maintain for the retransmission the MCS selected by the ACM strategy for the original transmission. In fact, in Chase combining the same FEC code is used for all consecutive retransmissions of a certain packet, so that each one of them is also selfdecodable, as it is possible for a receiver without soft values memory to decode each packet.

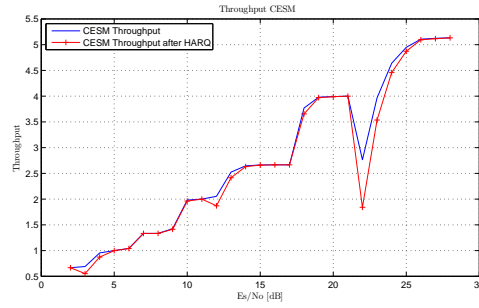
Incremental redundancy In Type II HARQ, in general different FEC codes are used between consecutive retransmissions and the receiver combines the received L-values of each retransmitted packet. A common implementation strategy is to transmit different parity bits in the consecutive retransmissions, which are combined in the receiver before decoding. In [14] it is shown that using a systematic mother FEC code, with a mother rate different from the initially selected R_2 , has significant benefits in terms of throughput and delay, especially if the first one is lower.

We have examined a particular Type II HARQ scheme, that is the one proposed in [22], and it is called *cyclic incremental redundancy* (CIR). This strategy generalizes the classical incremental redundancy scheme as the retransmission scheme sends at each retransmission a certain number of coded bits in a cyclic fashion. The inherent advantage of using such a scheme is that there is no restriction on the number of the retransmitted coded bits, as the retransmission unit can be varied depending on the necessity.

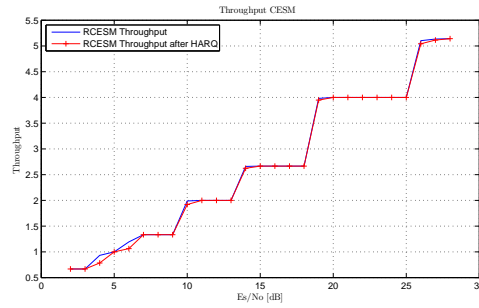
4.2.1 Retransmission results

Applying retransmission with our hypothesis of perfect channel state information has the constraint of being an unrealistic evaluation. In fact, applying the simplest strategy of Chase combining we find that it is required only one retransmission in the majority of the cases and that the resulting throughput doesn't show a big

difference with that one obtained before, as depicted in Figure 4.10. This can be



(a) WER



(b) Throughput

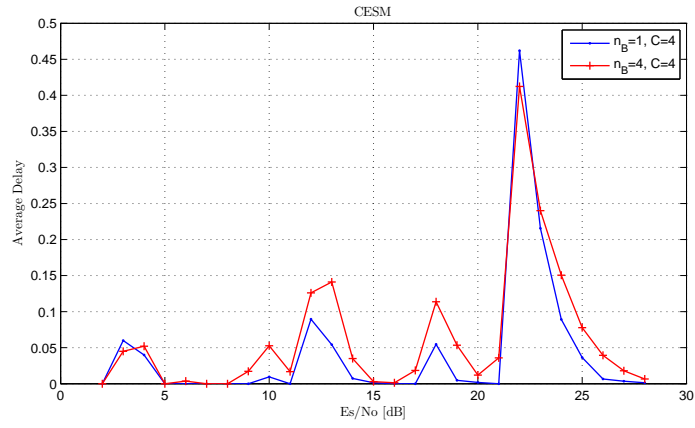
Figure 4.10: Throughput comparison before and after the retransmission when applying CESHM 4.10(a) and RCESHM 4.10(b)

explained taking into account that we don't have any channel prediction error, that usually has to be considered in these evaluation on HARQ as in [14]. For this reason we limit ourselves to evaluate the performances in terms of delay only for the Chase combining scheme, as with those simplified assumptions there wouldn't rise significative advantages in the implementation of incremental redundancy.

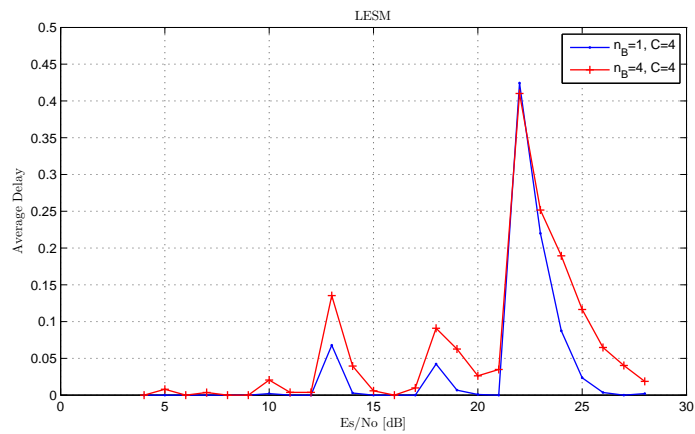
Applying Type I HARQ allows us to finally decode correctly all the transmitted codewords. In this last analysis we want to evaluate the delay resulting from this technique, calculating it as the number of required retransmission for each SNR, averaged on the total number of transmitted codewords.

In Figure 4.11 are shown the delays corresponding to the retransmission of the incorrectly received codewords of figures 4.3, 4.7 and 4.8. The CESHM and LESM methods, that have undesired picks of WER over 1%, give rise to quite high delays that reach even 45%. On the contrary, the RCESHM results in quite lower delays, with a maximum 6%. Therefore, also in this approximated analysis, the RCESHM

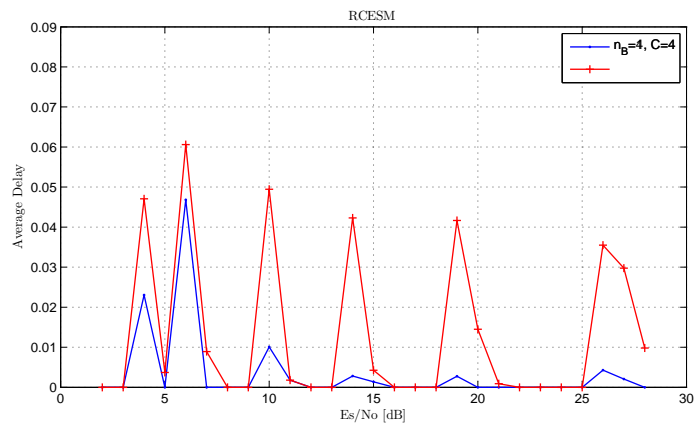
confirms its good potentialities.



(a) retransmission delay using CESM, $n_B = 1, 4$



(b) retransmission delay using LESM, $n_B = 1, 4$



(c) retransmission delay using RCESM, $n_B = 1, 4$

Figure 4.11: Delay calculated as number of retransmission for each used ESM method

Chapter 5

Conclusions

Link adaptation (LA) is nowadays one of the crucial techniques that allows wireless communications to provide users with a flexible, reliable and high speed connection, as the demand for broadband systems is continuously growing. The goodness of the reachable performances is based on an accurate estimate of the word error rate resulting from certain channel conditions. The link performance model that provides us with such an estimate is the effective SNR mapping (ESM) that takes into account the channel characteristics as well as the transmission parameters.

In this thesis we have investigated how to improve the performances of this technique, with the goal of defining a simple and fast criterium that provides a reliable estimate to use in the link adaptation. Therefore, we have defined a doubly-selective channel model to take into account the variation of the experienced conditions from subcarrier to subcarrier and from OFDM symbol to symbol. Our purpose was to obtain a sub-optimal evaluation of the various method's performances, neglecting the correcting factor that usually has to be configured carefully to get very accurate estimates. With this assumption, the existent ESM methods have been evaluated in our context, resulting in the strong need of such a scaling parameter to guarantee good performances.

In particular, the CESM method can be considered a good link performance model unless a little bias constraints the result to an underestimate and thus causes the wrong selection of the MCS by the ACM algorithm. On the contrary, if not corrected with a heavy scaling factor, the exponential SNR mapping overestimates a lot the real WER trend and therefore, in our analysis, cannot be considered an efficient model, as it results in an extremely low throughput. Nevertheless we can state that this method can be a promising solution for the ESM issue if appropriate correcting

factor is defined.

Another investigated method is the logarithmic ESM (LESM) that shows very interesting performances, with a quite accurate match, but presents clearly a slope different from the real WER's once. This facts causes the shift from a desirable overestimate to an underestimate that gives unacceptable results in link adaptation.

A new link performance model has been proposed using the CESM concept with the assumption of the Rayleigh fading channel. This approach led to use the Rayleigh channel capacity non-closed formula as the ESM metric and for this reason we called this method RCESM. The estimate results show desirable characteristics of minimum scattering and deviation, especially for a perfectly frequency interleaved channel.

Other two mapping methods based on the weighted mean have been proposed, but their performances depend strongly on the particular channel realization and therefore they cannot be considered a valid alternative to the ESM methods.

All those considerations have been confirmed by realistic simulations of the link adaptation scheme. Moreover, Type I HARQ, also called Chase combining, has been implemented to complement the link adaptation scheme where its performances were unsatisfactory. The LA WER results are coherent with what expected for each method and in particular, the proposed RCESM method shows interesting good performances, in our suboptimal context, when the QAM symbols experience a completely uncorrelated channel. This situation can be reproduced in every transmission system, independently of the channel characteristics, by simply including a frequency interleaver. We then conclude our analysis of metrics for the link performance model with some possible open issues regarding the calibration of the EESM method, the inclusion of the RCESM with a proper system model and the investigation of the joint usage of link adaptation and hybrid HARQ.

Ringraziamenti

Giunta alla conclusione del mio percorso di studi e con essa all'inizio della vita lavorativa vera e propria, mi guardo indietro e vedo le persone che mi hanno accompagnato lungo questa strada.

Primi fra tutti, i miei genitori, ai quali va il più grande dei ringraziamenti, per avermi insegnato a vivere così come a studiare e soprattutto per l'incondizionata fiducia che mi ha permesso di affrontare tutte le sfide fin ora incontrate.

Allo stesso modo, ringrazio i miei nonni, anche quelli che non mi possono vedere in questo momento che, sono sicura, li avrebbe riempiti di gioia, così come in loro io trovo tutt'ora l'ispirazione per la gioia di vivere.

Non possono poi mancare i miei inseparabili compagni di studio. Grazie a Stella per il sempre presente entusiasmo, capace di risollevare una intera giornata di conti neri. Ad Alice, per l'esempio che mi ha dato giorno dopo giorno di determinazione nello studio e nell'amicizia. Mi mancheranno poi i confronti su temi di scienza e di vita con Vincenzo.

Un grazie particolare va a France, che oltre a sopportarmi in questi mesi all'estero nei momenti di pessimismo, mi è stato vicino in quelli realmente difficili, dandomi un forte appoggio sia tecnico che morale.

Vorrei poi ringraziare il Professor Luise, non solo per avermi dato la possibilità di fare questa esperienza al CTTC di Barcellona, ma anche per l'immane disponibilità e soprattutto per avermi appassionata con i suoi insegnamenti nel modo più sano al mondo delle telecomunicazioni.

Grazie infine a tutte quelle persone che non ho citato, ma che in questi anni mi sono state vicine con il loro affetto e con la loro amicizia.

List of Figures

| | | |
|-----|--|----|
| 2.1 | Transmission system model | 6 |
| 2.2 | Equivalent block scheme of the transmitter | 11 |
| 2.3 | Rayleigh probability distribution function with $\sigma = \frac{1}{\sqrt{2}}$ | 12 |
| 2.4 | Fitting between analytical approximation and simulation results of the WER for AWGN channel | 16 |
| 2.5 | Fitting between analytical approximation and simulation results of the WER for Rayleigh fast fading channel | 16 |
| 2.6 | Fitting between analytical approximation and simulation results of the WER for Rayleigh slow fading channel | 17 |
| 3.1 | | 20 |
| 3.2 | Interpolation with $\gamma_{eff} < \bar{\gamma}$ | 21 |
| 3.3 | Interpolation with $\gamma_{eff} > \bar{\gamma}$ | 21 |
| 3.4 | CESM performances for QPSK, 16QAM and 64QAM with $R_2 = 0.5$ and $n_B = 1, 4$. Dashed lines represent the AWGN and Rayleigh theoretical curves for each modulation | 24 |
| 3.5 | EESM performances for QPSK, 16QAM and 64QAM with $R_2 = 0.5$ and $n_B = 1, 4$. Dashed lines represent the AWGN and Rayleigh theoretical curves for each modulation | 26 |
| 3.6 | LESMS performances for QPSK, 16QAM and 64QAM with $R_2 = 0.5$ and $n_B = 1, 4$. Dashed lines represent the AWGN and Rayleigh theoretical curves for each modulation | 27 |
| 3.7 | RCESM performances for QPSK, 16QAM and 64QAM with $R_2 = 0.5$ and $n_B = 1, 4$. Dashed lines represent the AWGN and Rayleigh theoretical curves for each modulation | 30 |
| 3.8 | exponential distribution with $\bar{\gamma} = 1$ | 31 |

| | | |
|------|--|----|
| 3.9 | DWM and IWM performances for QPSK, 16QAM and 64QAM with $R_2 = 0.5$ and $n_B = 1, 4$. Dashed lines represent the AWGN and Rayleigh theoretical curves for each modulation | 33 |
| 3.10 | Performances of CESM method over QPSK on channel model with $n_B = 1$ 3.10(a), $n_B = 4$ 3.10(b); 16QAM with $n_B = 1$ 3.10(c), $n_B = 4$ 3.10(d); 64QAM with $n_B = 1$ 3.10(e), $n_B = 4$ 3.10(f). $R_2 = \frac{1}{2}$ | 36 |
| 3.11 | Performances of EESM method over QPSK on channel model with $n_B = 1$ 3.11(a), $n_B = 4$ 3.11(b); 16QAM with $n_B = 1$ 3.11(c), $n_B = 4$ 3.11(d); 64QAM with $n_B = 1$ 3.11(e), $n_B = 4$ 3.11(f). $R_2 = \frac{1}{2}$ | 38 |
| 3.12 | Performances of LESM method over QPSK on channel model with $n_B = 1$ 3.12(a), $n_B = 4$ 3.12(b); 16QAM with $n_B = 1$ 3.12(c), $n_B = 4$ 3.12(d); 64QAM with $n_B = 1$ 3.12(e), $n_B = 4$ 3.12(f). $R_2 = \frac{1}{2}$ | 40 |
| 3.13 | Performances of RCESM method over QPSK on channel model with $n_B = 1$ 3.13(a), $n_B = 4$ 3.13(b); 16QAM with $n_B = 1$ 3.13(c), $n_B = 4$ 3.13(d); 64QAM with $n_B = 1$ 3.13(e), $n_B = 4$ 3.13(f). $R_2 = \frac{1}{2}$ | 41 |
| 3.14 | Performances of IWM method over QPSK on channel model with $n_B = 1$ 3.14(a), $n_B = 4$ 3.14(d); 16QAM with $n_B = 1$ 3.14(b), $n_B = 4$ 3.14(e); 64QAM with $n_B = 1$ 3.14(c), $n_B = 4$ 3.14(f). $R_2 = \frac{1}{2}$ | 42 |
| 3.15 | Performances of DWM method over QPSK on channel model with $n_B = 1$ 3.15(a), $n_B = 4$ 3.15(d); 16QAM with $n_B = 1$ 3.15(b), $n_B = 4$ 3.15(e); 64QAM with $n_B = 1$ 3.15(c), $n_B = 4$ 3.15(f). $R_2 = \frac{1}{2}$ | 43 |
| 4.1 | Throughput of the seven MCS over AWGN and Rayleigh fading channels | 46 |
| 4.2 | Link adaptation thresholds for the corrsipondent WER set of a Gaussian channel | 47 |
| 4.3 | Link adaptation with CESM: resulting WER and throughtup for $n_B = 1$ and different frame lengths | 49 |

| | | |
|------|---|----|
| 4.4 | Link adaptation with CESM: resulting WER and throughput for $n_B = 4$ and different frame lengths | 50 |
| 4.5 | Efficiencies plan with link adaptation results using CESM on a AWGN channel | 51 |
| 4.6 | Link adaptation with EESM: resulting WER and throughput for $n_B = 1, n_B = 4$ and frame length of $C = 4$ | 52 |
| 4.7 | Link adaptation with LESM: resulting WER and throughput for $n_B = 1, n_B = 4$ and frame length of $C = 4$ | 53 |
| 4.8 | Link adaptation with RCESM: resulting WER and throughput for $n_B = 1, n_B = 4$ and frame length of $C = 4$ | 54 |
| 4.9 | Efficiencies plan with link adaptation results using RCESM on a AWGN channel | 55 |
| 4.10 | Throughput comparison before and after the retransmission when applying CESM 4.10(a) and RCESM 4.10(b) | 58 |
| 4.11 | Delay calculated as number of retransmission for each used ESM method | 60 |

List of Tables

| | | |
|-----|--|----|
| 2.1 | MCS set specification | 9 |
| 2.2 | $\gamma_0^{(c)}$ and $\alpha^{(c)}$ values for AWGN and Rayleigh channel | 15 |

Bibliography

- [1] B. Gage, C. Martin, E. Sich, W. Tong “Focus on broadband wireless access” Nortel technical journal
- [2] J. F. Hayes “Adaptive feedback communications”, *IEEE Trans. Commun.*, Vol. 16, No. 1, pp. 2934, Feb. 1968.
- [3] A. Goldsmith “Wireless Communications”, Cambridge University Press, 2005 cap. 9
- [4] Yan Li, W. E. Ryan “Mutual-Information-Based Adaptive bit-loading algorithms for LDPC-coded OFDM” *IEEE Trans. Commun.*, Vol. 6, No. 5, May 2007.
- [5] J. Huang, R. A. Berry, M. L. Honig “Wireless Scheduling With Hybrid ARQ”, *IEEE Trans. Commun.*, Vol. 4, No. 6, Nov. 2005.
- [6] J. A. C. Bingham, “Multicarrier modulation for data transmission: an idea whose time has come”, *IEEE Commun. Mag.*, vol. 28, pp. 5-14, May 1990
- [7] G. Caire, G. Taricco, and E. Biglieri, “Bit-interleaved coded modulation,” *IEEE Trans. Inform. Theory*, vol. 44, pp. 927946, May 1998.
- [8] ST-2003-50707581 WINNER, “D2.10: Final report an identified RI key technologies, system concept, and their assessment, Dec. 2005.
- [9] ETSI EN 301 790 V1.4.1 (2005-09), “Digital Video Broadcasting (DVB); Interaction channel for satellite distribution systems, Sept. 2005.
- [10] A. Banerjee, D. J. Costello, T. E. Fuja, P. C. Massey “Bit Interleaved Coded Modulation Using Multiple Turbo Codes”, *Information Theory, 2002. Proceedings. 2002 IEEE International Symposium on Information Theory*

- [11] S.Pfletschinger, A. Piatyszek, S. Stiglmayr “Frequency-Selective Link Adaptation using Duo-Binary Turbo Codes in OFDM Systems”
- [12] T. Ekman “Prediction of Mobile Radio Channels Modeling and Design” PhD Thesis, Uppsala University, ISBN 91-506-1625-0 Oct. 2002, 254 pp.
- [13] M. Martinez Navarro. “Performance Analysis of GPRS Coding Schemes”. Aalborg University, August 1999
- [14] S.Pfletschinger, M. Navarro “Link adaptation with retransmissions for partial channel state information” Submitted to Globecom 2008
- [15] Louay Jalloul “IEEE 802.16m Evaluation Methodology Document (EMD)” IEEE 802.16m-08/004r2 section 4
- [16] Esa Tuomaala, Haiming Wang “Effective SINR approach of link to system mapping in OFDM/multi-carrier mobile network” Mobile Technology, Applications and Systems, 2005 2nd International Conference Nov. 2005
- [17] Brueninghaus, Astdlyt, Silzert, Visuri, Alexiou⁵, Karger, Seraji “Link Performance Models for System Level Simulations of Broadband Radio Access Systems” 2005 IEEE 16th International Symposium on Personal, Indoor and Mobile Radio Communications
- [18] Ericsson. “Effective SNR mapping for modelling frame error rates in multiple-state channels”. 3GPP2-C30-20030429-010, April 2003
- [19] Paunov, Camargo, Czylik “EESM as a Link to System Level Interface for MIMO Systems based on QOSFBC” Intl. ITG/IEEE Workshop on Smart Antennas (WSA 2007), vol. 1, pp. 2630, Mar. 2007
- [20] Kan Zheng; Yuan Gai; Guoyan Zeng; Wenbo Wang “Performance comparison of interleaving methods in joint frequency-time spreading OFDM-CDMA” International Conference on Communications, Circuits and Systems, 2004. ICCAS 2004. 2004 Volume 1, 27-29 June 2004 Page(s):334 - 338 Vol.1
- [21] Frenger, Parkvall, Dahlman “Performance Comparison of HARQ with Chase Combining and Incremental Redundancy for HSDPA” Vehicular

Technology Conference, 2001. VTC 2001 Fall. IEEE VTS 54th Volume 3, Issue , 2001 Page(s):1829 - 1833 vol.3

- [22] S. Pfletschinger *et al.*, “D2.2.3 modulation and coding schemes for the WINNER II system,” IST-4-027756 WINNER II, Tech. Rep., Nov. 2007